



Phytomediated zinc oxide and sulfur nanoparticles for management of soft-rot causing pathogenic fungi in ginger

Pramod U. Ingle^a, Mahendra Rai^{a,b}, Patrycja Golińska^c, Aniket K. Gade^{a,c,d,*}

^a Nanobiotechnology Laboratory, Department of Biotechnology, Sant Gadge Baba Amravati University, Amravati, Maharashtra, India, 444602

^b Department of Chemistry, Federal University of Piauí (UFPI), Teresina, Brazil

^c Department of Microbiology, Nicolaus Copernicus University, 87-100 Torun, Poland

^d Department of Biological Sciences and Biotechnology, Institute of Chemical Technology, Nathalal Parekh Marg, Matunga, Mumbai, Maharashtra, India, 400019

ARTICLE INFO

Handling Editor: Dr. Ching Hou

Keywords:

Nanofungicides

Pythium

Fusarium

Aspergillus

Zone of inhibition

Minimal inhibitory concentration

ABSTRACT

Diseases management has been the greatest challenge to agriculture leading to huge crop failure, represented in low-profit production. Phytopathogenic fungi are among pathogens causing a variety of agricultural diseases. Various nanoparticles (NPs) have previously been employed to combat phytopathogenic fungi. Post-harvest deterioration due to fungal invasion is the most imperative cause of loss of ginger (*Zingiber officinale*) production. In the present study, four fungal pathogens isolated from soft-rot infected ginger were identified as *Pythium* spp. (isolate I and II), one *Fusarium* sp. (isolate III) and one *Aspergillus* sp. (isolate IV). *Moringa oleifera* mediated zinc oxide (ZnONPs) and sulfur nanoparticles (SNPs) were characterized by UV–Visible spectrophotometry and showed absorption maxima at 356 nm and 295 nm. Average size of NPs under Nanoparticle Tracking Analyzer was 78 nm and 26 nm respectively, confirmed by FESEM. Stable NPs with zeta potential of -14.1 mV (Standard deviation = 4.51 mV) and -21.1 mV (Standard deviation = 9.56 mV) were synthesized. FTIR detected the presence of various functional groups in NPs. *In vitro* antifungal activity was assessed by Kirby-Bauer disc diffusion assay and MIC values compared to antibiotic ketoconazole and fungicide mancozeb. Time kill assay represented the minimum time required by selected NPs to inhibit the growth of test pathogenic fungi. ZnONPs and SNPs can be used for further antifungal studies in the field as novel nanofungicides. Extrapolated and uncontrolled use can lead to the inhibition of germination, reduction in photosynthesis rate, and disruption of the plant roots. Thorough small-scale experimentation is necessary before commercialization.

1. Introduction

Ginger (*Zingiber officinale* Rosc.) (Family: Zingiberaceae) is a perennial herb. The ginger rhizomes are consumed as a spice. India being a foremost producer of ginger, during 2012–13 the production in country was 7.45 lakh tonnes of ginger from 157,839 ha area. Ginger is cultivated in almost all the states in India. However, states mainly Karnataka, Meghalaya, Orissa, Arunachal Pradesh, Assam, and Gujarat contribute 65% to the country's production (ICAR- IISR, 2013; IISR-Annual ICAR-IISR-Annual Report, 2022).

* Corresponding author. Nanobiotechnology laboratory, Department of Biotechnology, Sant Gadge Baba Amravati University, Amravati, Maharashtra, India – 444602.

E-mail addresses: aniketgade@sgbau.ac.in, aniket.gade@umk.pl, ak.gade@ictmbai.edu.in (A.K. Gade).

<https://doi.org/10.1016/j.bcab.2024.103229>

Received 1 February 2024; Received in revised form 1 May 2024; Accepted 13 May 2024

Available online 17 May 2024

1878-8181/© 2024 The Authors. Published by Elsevier Ltd. This is an open access article under the CC BY-NC license (<http://creativecommons.org/licenses/by-nc/4.0/>).

Ginger is an essential spice crop in India and world as well. Besides its use in preparation of curry recipes, ginger is widely used in processed and unprocessed foods, medicines and cosmetic products. Ginger as a nutraceutical product is used in the pharmaceutical and food industries for a long time. Growing health concerns among all classes of people and awareness on the use of ginger in pharmaceutical products, the demand for organic as well as value-added ginger is increasing with time. Ginger is mostly cultivated by the marginal and small farmers in India and it is cultivated in small patches of land. Potential increase in ginger production in the country is needed for changing the socio-economic situation of a section of people through ginger farming (NAIP, 2014). Globally, many countries are also facing problems during the cultivation and post-harvest storage and maintenance of ginger. In the case of country like Ethiopia, due to higher chances of fungal attacks, production of ginger is lowered. There are few varieties available around the world, limiting their extensive species based yield development studies. Majority of the cultivation methods are conventional accompanied by the recent intrusion of bacterial wilt in the agricultural field (Zakir et al., 2018; Kifile et al., 2023). Sri Lanka being a minor producer of ginger, land availability has always been a constraint. In addition, marketing issues, unavailability of quality seeds, higher inputs values, scarcity of knowledge of cultivation and proper procedures of post-harvest handling and storage unfortunately limit the ginger production (Adeboye, 2011; Dewanarayana and Wimalaratana, 2018).

Post-harvest damage and decay are the most significant reasons for the loss of *Zingiber officinale* production which is mainly due to fungal attack. Various *Pythium* spp. and the *Fusarium* spp. are the major phytopathogenic fungi causing soft-rot in ginger (Sharma et al., 2022; Tilahun et al., 2022; Nejad et al., 2023). Despite the lack of recent data, during the year 2012–2013 the country produced 0.745 million tons of ginger from 157,839 ha of land (Jayashree et al., 2016; Prasath et al., 2023). Plant pests and pathogens cause projected worldwide losses of 20%–40% per year (Flood, 2010). Thus, there is an increased motivation to develop high-performance and cost-efficient, control agents that are less toxic to the environment. Fungi are the main cause of post-harvest deterioration in ginger. Post-harvest spoilage of ginger can be reduced by proper growing methods, harvesting, and post-harvest handling techniques. The aforementioned problems with ginger production can be addressed with the development of nanotechnology. Nanotechnology in agriculture is presently being explored in the delivery of plant hormone, water management, seed germination, targeted gene transfer, nanobarcoding, nanosensors, and controlled release of agrichemicals. Researchers have engineered nanoparticles (NPs) with anticipated properties, such as pore size, shape, and surface functionalities, to use them as protectants or for targeted and precise dissemination via encapsulation, adsorption, and/or conjugation of a dynamic ingredient, such as a pesticide (Khandelwal et al., 2016; Hayles et al., 2017; Mahmud et al., 2023; Nevado-Velasquez et al., 2023). A new generation of fungicides is being developed in agricultural nanotechnology that has potential to manage plant diseases. The most usually explored nanoparticle carriers are silica, polymer mixes, and chitosan. Various fungi are continuously tested for antifungal efficacy of the nanofungicides against them (Worrall et al., 2018; Yadav et al., 2023a).

Amid the different microbial pathogens, phytopathogenic fungi are main cause of potent diseases in agriculture. Fungi easily adopt with any medium and are capable of growing different substrates or media in precarious environmental surroundings. They can disturb different growth stages of the crop, right from sowing to vegetative and from production to postharvest. Today, phytopathogenic fungi are controlled with chemical fungicides, which are costlier and can be obtained from the market. They have resulted the development of fungi with more resistance, becoming sturdier against chemical products. However, their undiscerning use have created several problems such as pollution of environmental factors, diseases in animals and humans, and ecological imbalances. Such as, aquatic habitats are contaminated via wastewater and agriculture use discharges. While the non-point sources like drift, drainage and surface run-off can cause water pollution (Bereswill et al., 2012; Zubrod et al., 2019). In case of wetlands, removal efficacy of fungicides also plays a vital role in damaging environment (Gikas et al., 2022).

Traditional methods of controlling mycological infections in ginger crop includes chemical methods, physical methods, and biological methods. The physical method involves suppressive soil with higher clay content and lower pH for cultivation, mulching of soil via soil solarization, covering moist fields with plastic sheets, followed by phyto-sanitization (Bennett et al., 1991; Chérif et al., 1994; Dake, 1995; Rai et al., 2018). Chemical method applies various synthetic fungicidal chemical agents like metalaxyl (fosetyl-aluminum/Ridomil), Apron 35 WS, Dithane M 45, or their combination as Chloropyrifos 20 EC + Mancozeb 80 W P (Diathane M-45) and Carbendazim 50 DF (as Bavistin) for synergistic activity (Luong et al., 2010; Gautam and Mainali, 2016; Rai et al., 2018). Biological approaches includes the application of plant extracts like *M. oleifera*, *Azadiracta indica*, *Aegel marmelos*, etc. For controlling ginger soft-rot (Parveen and Sharma, 2014). Various bacterial species like *Bacillus*, *Rhizobium*, *Pseudomonas*, etc. and fungal species like *Fusarium* and *Trichoderma* are used as biocontrol agents in ginger soft-rot management (Yadav et al., 2023a). *M. oleifera* leaf and seed extracts has been reported for its fungistatic potential against many crop pathogenic fungi like *Botrytis cinerea* (He et al., 2011; Ahmadi et al., 2021). Also, the NPs synthesized using *M. oleifera* extracts reduce the radial growth of fungi (Jenish et al., 2022). These studies imposed a choice of moringa for the production of NPs in the present study.

Nanotechnology offers an alternate eco-friendly method for plant disease management and overcomes drawbacks associated with ecotoxicity. Plant-based synthesis methods are called as green technologies as they are less polluting, cost-effective, helps in ensuring human health and environmental safety (Ying et al., 2022). Nanomaterials can increase crop development and yields, improve identification and management of pests and diseases, helps in genetic modification of plants, and ease in postharvest managements (Ghidan and Al Antary, 2020). Active agrochemicals are delivered in agriculture fields in a smart way using nanotechnology (Gogos et al., 2012). Thus, sustainably strengthen the new paradigm in agriculture and alleviate prevailing complexities (Fraceto et al., 2016). Various NPs are applied in agriculture, and their use depends upon their mode of action. The most widely used NPs are silver, titanium, gold, copper, zinc, aluminum, chitosan, silica, and sulfur (Ghazy et al., 2021; Banerjee and Rajeswari, 2024; Sabir et al., 2014; Mustafa et al., 2023; Sivakumar et al., 2024). There is a need of a sustainable product with antifungal activity with minimal losses of the product and the least damage to the environment. Nanotechnology provides a sustainable and advanced approach to replace conventional fungicides with biogenic nanoparticles. The present study encompasses the *in vitro* evaluation of zinc oxide and sulfur NPs

against fungal pathogens in ginger and their management (Tandon et al., 2023). The present study will play an important role in management of plant pathogenic fungi and related infections based upon the plant mediated nanoparticles in a sustainable way, and with future studies aimed at developing nano-based antifungal formulation for agriculture application.

2. Materials and methods

2.1. Survey and sample collection

A market survey was made alongside the field survey in pursuit of soft-rot infected ginger for isolation of fungal pathogens. The infected ginger samples were collected from the street vendors and agro-food markets of Amravati district. Some ginger samples were collected from the nearby agricultural fields of farmers (Location coordinates: 20° 56' 14.7264" N and 77° 46' 46.3764" E). In total about 35 samples of ginger were collected. The ginger samples were further subjected to surface cleaning and fungal pathogen isolation and identification as mentioned in section 2.2.

2.2. Isolation and morphological identification of fungi

Ginger rhizome samples (100 g) were washed with sterile distilled water followed by surface sterilized by using 0.1 % sodium hypochlorite for 3 min and followed by three times successive sterile distilled water washes. Ginger samples were washed with sodium hypochlorite to remove any bacterial contaminants on the ginger surface that could interfere with the isolation of fungal pathogens from inside the ginger. The samples were chopped into small, thin slices of 1–2 mm thickness with the help of a sterile knife or a scalpel. The ginger slices were aseptically inoculated onto a Potato Dextrose Agar (PDA) (pH, 5.6) using sterile forceps. The plates were incubated for 4 days at 25 °C. When the mycelia arise, the organisms were sub-cultured on fresh sterile agar media to get a pure culture of each isolate.

Ginger decomposing fungi were isolated and identified by microscopy (Fig. 1). Seven to fifteen-day-old fungal cultures grown on PDA were aseptically taken using sterile inoculating needle, mounted on to clean microscopic slide and stained using lactophenol cotton blue (HiMedia, Mumbai, India). Identification of fungi was carried out to the genus level based on morphological characteristics using compound microscope and colony characteristics on PDA and compared with structures in Samson et al. (2009) and Dugan (2006) and colored plates in Samson et al. (2009).

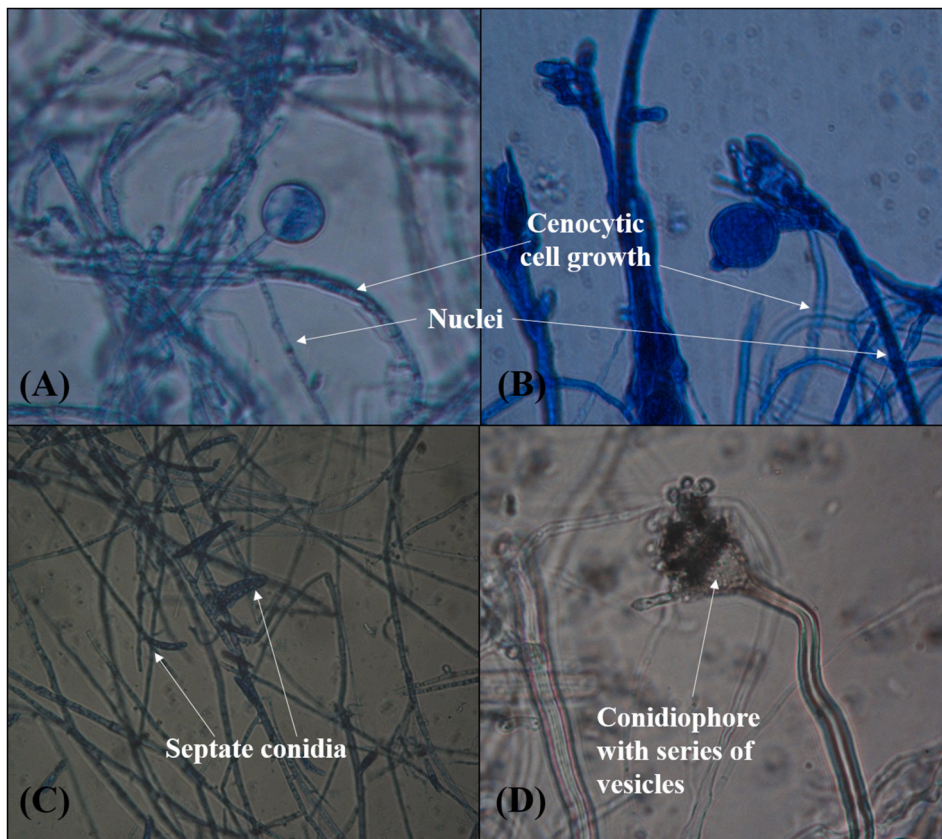


Fig. 1. Fungi isolated from soft-rot infected ginger, (A) *Pythium* isolate I, (B) *Pythium* isolate II, (C) *Fusarium oxysporum* isolate III, (D) *Aspergillus* isolate IV.

2.3. Preparation of aqueous *Moringa oleifera* leaf extract

Zinc oxide and sulfur NPs were synthesized from the aqueous *Moringa oleifera* leaf extract which was prepared from freshly harvested leaves. Fresh moringa leaves (10 g) were cleaned by multiple washing under running tap water trailed by surface sterilization with 5 % sodium hypochlorite for 2 min. The surface sterilized leaves were finally washed with sterile distilled water and kept for boiling in distilled water (100 ml) for 15 min with continuous stirring. The extract was cooled to room temperature, filtered through Whatman filter paper followed by passing through 0.2 μm nitrocellulose filter to get rid of any impurities. The final volume was made up with sterile distilled water to 100 ml and the resulting extract was stored at 4 °C for further use.

2.4. Synthesis of biogenic NPs zinc oxide NPs (ZnONPs) and sulfur NPs (SNPs)

The ZnONPs were synthesized by equal volumes of 10 mM ZnSO_4 with diluted (1:20) *M. oleifera* extract in distilled water. The reaction mixture was continuously stirred for 30 min at room temperature with the dropwise addition of 0.1 N NaOH. The reaction mixture was observed for the formation of off-white precipitate of ZnONPs. For SNPs synthesis 50 mM of sodium thiosulphate (Awad et al., 2015) was mixed with 100 ml of *M. oleifera* extract. Few drops of concentrated hydrochloric acid were added with continuous stirring for 30 min at room temperature or until pale yellow precipitate of SNPs was observed. The precipitates for both ZnONPs and SNPs were purified by centrifugation at 15,000 rpm for 15 min at 4 °C. The pellet was washed multiple times to assure no impurities in the final product (El-Gebaly et al., 2024), followed by overnight drying of the pellet in oven at 40 °C.

2.5. Characterization of NPs

The *M. oleifera* mediated ZnONPs and SNPs were further detected in the colloidal form by visualization of any color change before and after synthesis. Characterization was done by UV–Visible spectrophotometry (NanoDrop, 2000c, Thermo Scientific, India; 1 mg/ml for both NPs, spectrum range 200–800, at room temperature) to determine absorbance maxima for respective NPs. The average size of NPs was determined using Nanoparticle Tracking Analyzer (NTA LM 20, Malvern, UK), which was further confirmed with FE-SEM (Field Emission Scanning Electron Microscopy, FESEM, JEOL JSM-7100 F, Singapore; 18 kV and 30,000 \times magnification) with dwell time of 6 μs for ZnONPs and 10 μs for SNPs. The stability based on the surface potential for NPs was determined by zeta potential measurements (Zetasizer Nano-ZS 90, Malvern, UK). The biochemical composition of the capping layer of ZnONPs and SNPs was elucidated by detecting the various functional groups exposed using Fourier Transform Infrared Spectrometry (FTIR Spectrometer, Bruker Optics ATR, GmbH, Germany). The purity of NPs and their crystalline or amorphous nature was predicted by X-ray diffraction studies (Rigaku X-ray diffractometer, USA). The percent elemental constitution of NPs was determined by EDX (Energy Dispersive X-ray Microanalysis) which confirms specimen composition and distribution of the NPs through spectrum and elemental mapping. The characterized ZnONPs and SNPs were further evaluated for their antifungal activity by various.

2.6. In vitro antifungal activity assessment

In vitro antifungal activity of ZnONPs and SNPs was evaluated against isolates of *Pythium* and *Fusarium* obtained from infected ginger samples by disc diffusion and Minimum Inhibitory Concentration (MIC) determination methods using microtiter plate assay as per guidelines of the Clinical Laboratory Standards Institute (CLSI, 2021) (<https://www.treata.academy/wp-content/uploads/2021/03/CLSI-31-2021.pdf>).

2.6.1. Kirby-Bauer Disc Diffusion assay

Kirby-Bauer Disc Diffusion susceptibility test was performed to determine whether the given test fungal culture is susceptible or resistant to the given set of NPs tested. Inoculum of all four isolates were prepared growing of fungal biomass on potato dextrose broth for 8–10 days which was suspended in Rosewell Park Memorial Institute medium (RPMI 1640 medium). The optical density (OD) was upheld between 0.15 and 0.17 at 530 nm. The fungal suspensions were spread with the help of a sterile cotton swab on sterile PDA plates. Sterile discs obtained from HiMedia (HiMedia Pvt. Ltd. Mumbai, Maharashtra, India) were positioned onto the surface of inoculated PDA plate. Each sterile disc was loaded with 20 μl of respective NPs (zinc oxide and sulfur) suspension (2 mg/ml for both the NPs). The precursor salts solutions ZnSO_4 (10 mM) and $\text{Na}_2\text{S}_2\text{O}_3$ (50 mM) were taken as a control set individually (same as used for the synthesis of NPs). A separate controls were maintained as water (a negative control), antifungal antibiotic ketoconazole and fungicide mancozeb (1 mg/ml) as a positive controls. Along with this a separate disc for diluted moringa leaf extract (1:20) and finally a blank disc was maintained with sterile distilled water. The activity of these NPs was assessed using diverse concentrations including 2 mg/ml. The plates were incubated for 24–48 h at 28 ± 2 °C till visible growth appeared. The zones of inhibition (ZOI) were measured in mm with scale. The experiment was accomplished in triplicate.

2.6.2. Determination of MIC by microdilution method

The MIC of NPs (zinc oxide and sulfur) was determined by micro-broth dilution method against all isolates. For evaluation of MIC, fungi were inoculated in potato dextrose broth (PDB) and incubated at 28 ± 2 °C for 7 days. The OD of the fungal suspension was attained between 0.15 and 0.17 by using RPMI medium. The absorbance was measured by using colorimeter at 530 nm and the fungal spore load was kept between 0.4×10^4 to 5×10^4 CFU/ml. The concentrations of NPs tested were in the range of 50–450 $\mu\text{g}/\text{ml}$ for both the NPs. 50 μl of fungal inoculum was added to each well. The negative control was maintained with sterile PDB broth to check sterility. Similarly, the positive control was maintained with PDB inoculated with 50 μl of fungal spore suspension with the standard fungicide i.e. mancozeb, 1 mg/ml. The micro dilution plates were incubated at 28 ± 2 °C for 3 days. The plates were observed at every 24 h interval. MIC recorded was the lowermost concentration of NPs that resulted in visual inhibition of fungal growth. Each assay was performed in triplicate.

2.6.3. Time kill assay

The fungal cultures were grown in PDB medium for 7 days to get visible growth. The nanoparticle concentration represented at MIC was taken to determine the minimum time required to inhibit 100 % of the fungal growth in liquid medium at 28 ± 2 °C. The fungal cultures treated with respective NPs for the time period of 60 h. An aliquot (10 μ l) was taken after every 6 h interval and spread on the PDA plate followed by counting the number of colonies after 3 days of incubation at 28 ± 2 °C. The plate showing the complete inhibition of fungal growth was selected for the respective treatment time as a minimum time of inhibition for the given set of fungus and nanoparticle treatment.

2.7. Statistical analysis

Statistical significance of the data obtained were analyzed and verified using the standard one way analysis of variance method (one-way ANOVA) for the test results for both the nanoparticles.

3. Results

3.1. Isolation and identification of fungi

The fungal isolates stained with lactophenol cotton blue were identified on the basis of their respective shapes of conidia and the respective genus for the given culture was determined. Isolate I and II grew as off-white colored colonies that showed the dark blue stained prominent nuclei and non-septate, cenocytic cell growth, which is a peculiar character of genus *Pythium*. *Pythium* isolates were identified on the basis of classification given by Patterson (1989) and Dick (2001). Isolates I and II were identified as *Pythium* spp. On the basis of their white colored colonies with irregular margins with radial growth pattern (Navi et al., 2019) and empty bur-siform sporangium with short exit tube (Fig. 1 A) and oogonium surrounded by several antheridia (Fig. 1 B) respectively (Ho, 2018). Isolate III was identified as *Fusarium oxysporum* (Fig. 1 C) (Leslie and Summerell, 2006) on the basis of fluffy growth and creamy white colored upper surface of colonies with slightly pink colored pigmentation at the bottom (Rafique et al., 2015). Conidiogenous cell was long and monophilides. Macroconidia were slender, slightly curved, showed 5-7 septations. Isolate IV was identified as *Aspergillus* sp. (Fig. 1 D) (Thom and Raper, 1945). Colonies showed green/yellow colored pigmentation and the bottom was shiny yellow to golden in color (Moslem et al., 2010; Awad et al., 2023). Microscopic structures showed flask-shaped phialides, with series of vesicles on the top of conidiophore (Raper and Fennell, 1965). The identified fungal cultures were maintained in a pure form on PDA medium and stored at 4 °C for further *in vitro* assessment.

3.2. Synthesis of biogenic NPs

The ZnONPs which were synthesized from *M. oleifera* leaf extract (Fig. 2 A) in the form of a white colloidal suspension (Fig. 2 B) which was collected by ultracentrifugation at 15,000 rpm for 10 min, followed by washing pellet with distilled water (3 times) and overnight drying in the oven at 40 °C. Off-white colloidal SNPs (Fig. 2 C) were also collected by centrifugation (15,000 rpm for 15 min) followed by washing with distilled water (3 times) and overnight oven drying to obtain the dry pellet. The dried pellets were ground in to a fine powder and collected in an air-tight vials for further characterization and *in vitro* assessment.

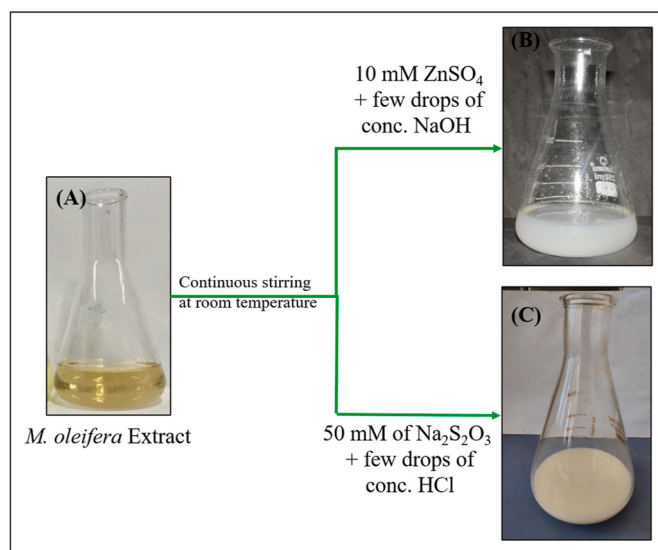


Fig. 2. Biological synthesis of nanoparticles from *M. oleifera* extract (A), white precipitate of Zinc oxide nanoparticles (ZnONPs) (B) and pale yellow precipitate of Sulfur nanoparticles (SNPs) (C). (For interpretation of the references to color in this figure legend, the reader is referred to the Web version of this article.)

3.3. Visual detection of nanoparticles

The aqueous *M. oleifera* extract which was pale yellow in color (Fig. 2 A) when mixed with the 10 mM zinc sulphate solution changed to the color to white precipitate of zinc oxide NPs (Fig. 2 B). This indicated the synthesis of ZnO NPs. The synthesis of sulfur NPs was confirmed by the formation of off-white precipitate (Fig. 2 C) of SNPs after the addition of sodium thiosulphate and a few drops of HCl to the moringa extract (Paralikar and Rai, 2018).

3.4. Characterization of NPs

3.4.1. Characterization of zinc oxide nanoparticles

UV-visible spectrophotometric measurement of ZnONPs indicated the absorbance maxima of 356 nm (Fig. 3 A). NTA analysis indicated the average size of 78 nm and 35 nm standard deviation with particle size distribution over a broad range (Fig. 3 B and 3 D). Particle concentration was found to be 1.5×10^7 particles/per ml of test sample. The zeta potential measurement indicated the average potential of -14.1 mV with the standard deviation of 4.51 mV (Fig. 3 C). The FTIR spectrometry indicated the peaks present for various functional groups exposed in the capping layer of ZnONPs (Fig. 4 A). The transmittance bands were observed at 3265 cm^{-1} which is assigned to O-H group in hydrogen bonded alcohols and phenols, 1722 cm^{-1} assigned to C=O group in aldehydes, ketones, carboxylic acids and esters. The peaks at 1565 cm^{-1} , 1320 cm^{-1} represented NO_2 group in nitro compounds. Transmittance peak at 1398 cm^{-1} was assigned to C-H stretch of alkanes. The minor peaks at 1153 cm^{-1} , 1025 cm^{-1} and 819 cm^{-1} represented C-N stretch of secondary amines, C-O stretch of ethers and esters and C-Cl stretch of aliphatic chloro compounds respectively. Energy dispersive x-ray analysis (Fig. 4 B) indicated the presence of 62 % of Zn by weight and 28.83 % by atomic weight, and rest was constituted by oxygen only. There were no other elemental impurities detected in EDX. X-ray diffraction pattern of ZnONPs (Fig. 4 C) showed Miller indices as 102, 110, 103 and 112 which corresponds to the 2 theta angle of diffraction of 47.51° , 56.53° , 62.83° and 67.89° . The Bragg's values and Miller indices indicated that the zinc oxide NPs were crystalline in nature with face centered cubic structure of ZnONPs crystals. FESEM of ZnONPs (Fig. 4 D) indicated the formation of polymorphic ZnONPs i.e. roughly circular and bar shaped ZnONPs crystals with size range in resemblance as per shown by NTA analysis. The roughly circular disc shaped crystal of ZnONPs have smooth but irregular margins with variable diameter ranging approximately between 10 and 60 nm. While bar shaped crystals are similar to quartz crystals with slender (with length 5–7 times the width) structure, fine edges and soft corners.

3.4.2. Characterization of sulfur nanoparticles

The sulfur nanoparticles (SNPs) indicated the absorption maxima at 295 nm under UV-visible light (Fig. 5 A). Average size of 52 nm was observed by NTA analysis with standard deviation of 32 nm (Fig. 5 B). The particle concentration was found to be 1.3×10^9 particles/per ml. The stable SNPs were confirmed by average zeta potential value of -21.2 mV and standard deviation of

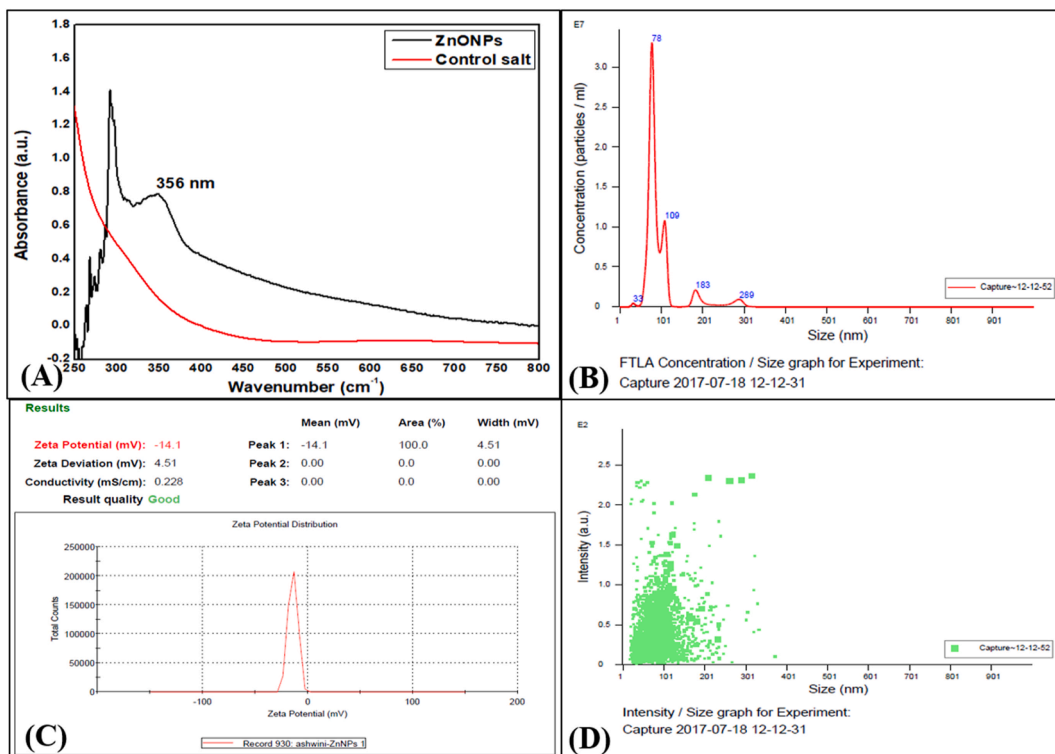


Fig. 3. Characterization of *M. oleifera* mediated ZnONPs, (A) UV-visible spectrum, (B) size determination using NTA (Nanoparticle Tracking Analysis), (C) Zeta potential determination, and (D) particle size distribution in 2D under NTA.

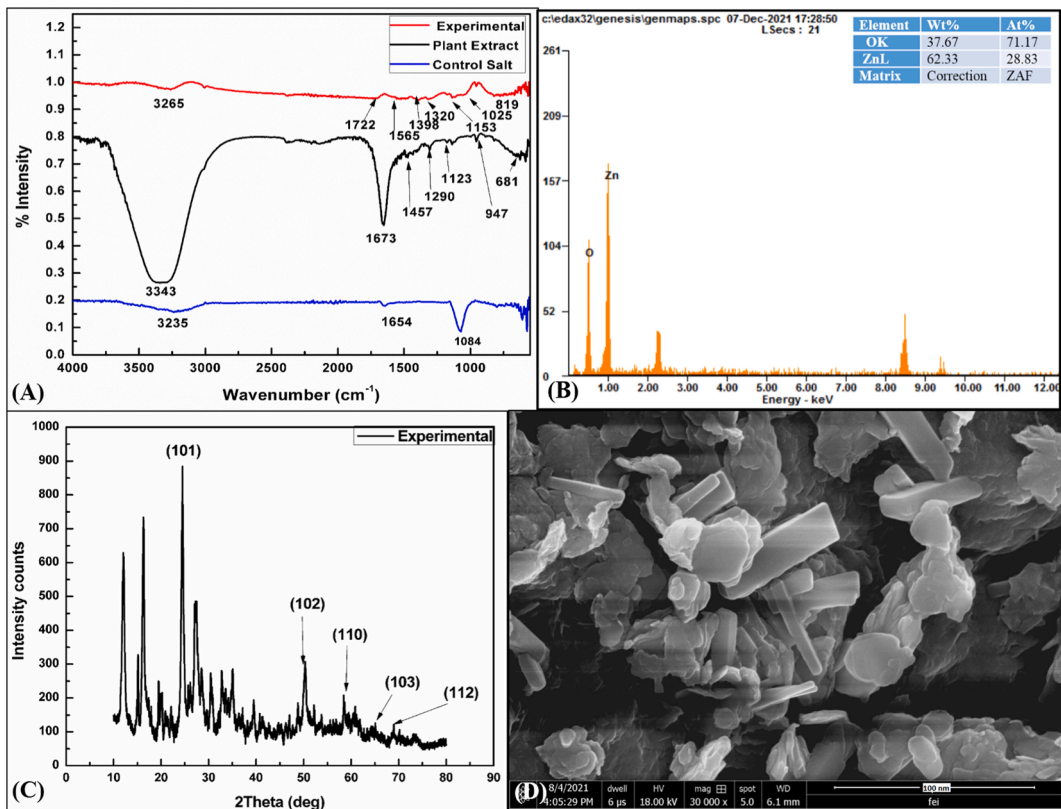


Fig. 4. Characterization of *M. oleifera* mediated ZnONPs, (A) Fourier Transform Infrared spectrum, (B) EDX pattern, (C) X-ray diffraction pattern, and (D) FESEM images.

9.56 mV (Fig. 5 C). The SNPs were observed to disperse over a broad range from 10 nm and up to 100 nm and very less particles with size above 100 nm (Fig. 5 D). The transmittance peaks were observed at 3412 cm^{-1} represented the presence of N–H stretch of amines and amides, 1644 cm^{-1} C=O groups of aldehydes and ketones, 1428 cm^{-1} C–H stretch of alkanes, 1251 cm^{-1} represented presence of C–N stretch of amines and amides. The other minor peaks at 1113 cm^{-1} , 986 cm^{-1} , 789 cm^{-1} and 652 cm^{-1} were assigned to C–O alcoholic stretch, C–H of alkenes, aliphatic chloro- and aliphatic iodo-compounds respectively were present in capping layer (Fig. 6 A). EDX represented the presence of sulfur (79.29 % by wt. And 65.63 % atomic weight) and oxygen only and no other elemental contamination (Fig. 6 B). XRD spectrum (Fig. 6 C) indicated the typical Miller indices for SNPs at 113 (15.38), 131 (22.68), 222 (23.07), 026 (25.83), 311 (27.71), 044 (31.39), 404 (37.35), 062 (42.78), 066 (47.88) and 517 (51.32). The miller indices were assigned to a specific Bragg's diffraction angle as given herewith. The Miller indices indicated the formation of face centered cubic crystalline SNPs (Joint Committee on Powder Diffraction, Standard file no. 04–0836). As shown in the figure (Fig. 6 D) FESEM disclosed the wrinkled with almost spherical sulfur NPs with polydispersed morphology with variable range of diameters were synthesized by *M. oleifera*. The size range of SNPs detected in FESEM corroborated with the NTA results. Some are slight ellipsoidal with rough or wrinkled surface. Accumulation of SNPs might have resulted in larger sized spheres as observed under FESEM.

3.5. *In vitro* antifungal activity assessment

In vitro antifungal activity of both the synthesized NPs namely zinc oxide and sulfur NPs were evaluated at concentrations 2 mg/ml, against two *Pythium* spp., *F. oxysporum* and *Aspergillus* sp. Isolated from infected ginger samples by Kirby–Bauer disc diffusion method (Bauer et al., 1966; Sales et al., 2016; Sharma et al., 2022).

3.5.1. Kirby-Bauer Disc Diffusion assay

The ZnONPs and SNPs post-characterization were evaluated for their antifungal activity against identified fungi by *in vitro* method i.e. Kirby-Bauer disc diffusion method. The diameter of zone of inhibition (ZOI) was measured, which determined the antifungal potential of test compound. The negative control sets viz. Plant extract (moringa leaf extract), sodium thiosulphate and zinc sulphate did not show any zone of inhibition against all four fungal cultures, indicating no antifungal activity exhibited by the precursor molecules used for the synthesis of NPs. The zones of inhibition for *Pythium* isolate I, were observed (Fig. 7) in the decreasing order as Mzb + ZnONPs > Mzb > Mzb + SNPs > Kz (ketoconazole) + SNPs > ZnONPs \approx Kz + ZnONPs \approx Kz > SNPs. For the *Pythium* isolate II, the order was observed as: Mzb + ZnONPs > Mzb \approx Mzb + SNPs \approx Kz + SNPs \approx Kz + ZnONPs > SNPs. Isolate III i.e. *Fusarium* sp. Showed highest ZOI by SNPs in combination with fungicide, mancozeb. The order of ZOI for *Fusarium* isolate was found in the order as: Mzb + SNPs > Mzb \approx Mzb + ZnONPs > Kz + SNPs \approx Kz + ZnONPs > SNPs \approx Kz > ZnONPs. Finally, the *Aspergillus* isolate

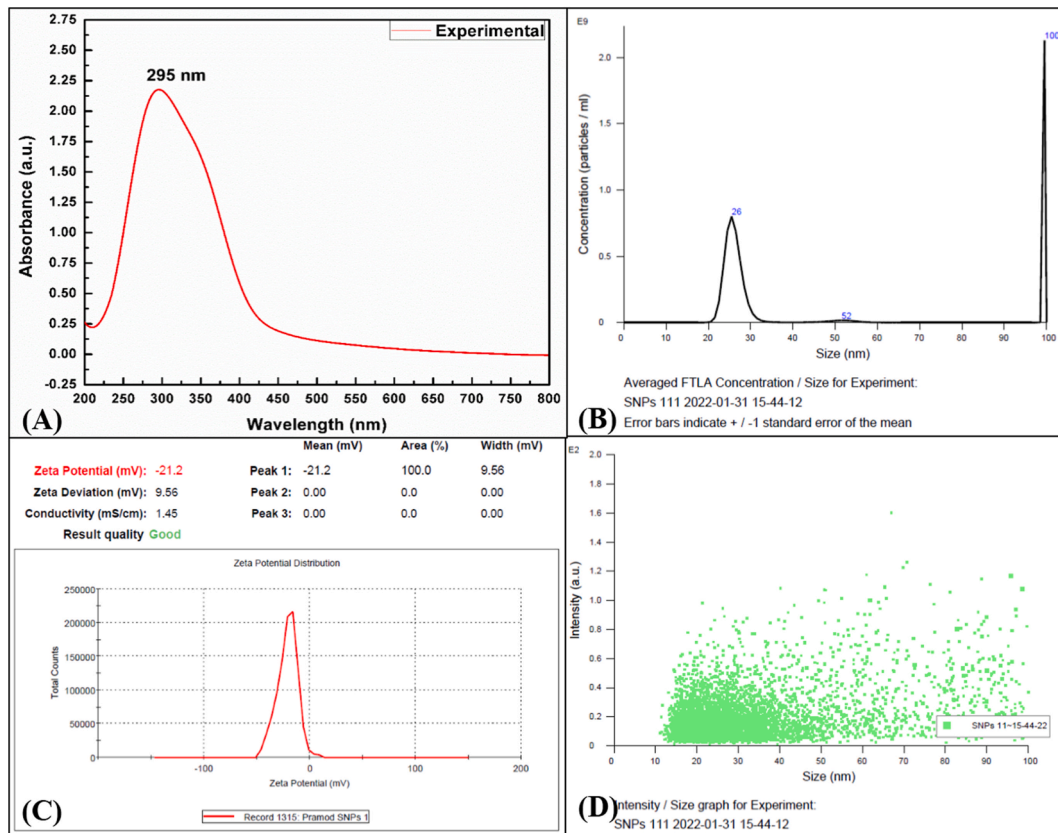


Fig. 5. Characterization of *M. oleifera* mediated SNPs, (A) UV-visible spectrum, (B) size determination using NTA (Nanoparticle Tracking Analysis), (C) Zeta potential determination, and (D) particle size distribution in 2D under NTA.

IV largest ZOI with SNPs in combination of antibiotic, ketoconazole which was equivalent to the ZOI shown by Mancozeb. The order of ZOI were found to be in the order as follows: Kz + SNPs \approx Mzb > Kz + ZnONPs > Kz > Mzb + SNPs > Mzb + ZnONPs > ZnONPs > SNPs. The smallest ZOI were observed for ZnONPs against, which might be the result of lower antifungal potential and less diffusion in medium from the sterile disc.

3.5.2. Determination of MIC by micro titer plate assay

The minimal inhibitory concentration for all test fungi were observed. ZnONPs showed the highest value of MIC against *Pythium* isolate I.e. 450 μ g/ml and lowest for the *Aspergillus* sp. *Pythium* II and *Fusarium* sp. Showed the same MIC values. SNPs showed the equivalent MIC against both *Pythium* isolate I and *Aspergillus* sp. The order of MIC followed by both ZnONPs and SNPs was observed as *Pythium* I > *Pythium* II \approx *Fusarium* sp. > *Aspergillus* sp. And *Pythium* I > *Aspergillus* sp. > *Pythium* II \approx *Fusarium* sp. Respectively (Supplenemary file, Fig. S1 – S4).

3.5.3. Time kill assay

The time of inhibition (TOI) of fungal growth at respective MIC was calculated for all selected fungi. The minimum treatment time of selected NPs was considered as TOI where no visible growth was observed after the given treatment time. In case of the treatment with biogenic ZnONPs treated set of fungi, a slow decrease in the viable spore count was observed up to \approx 18 h of incubation followed by rapid decline till \approx 36 h incubation (Supplementary file, Figs. S5 and S6). The complete growth was inhibited nearby \approx 42 h of incubation and no visible growth was observed at \approx 48 h PDA plates (Fig. 8). The complete inhibition of two isolates of *Pythium* (I and II), was observed at \approx 42 h, as no growth was observed on PDA plates. The *Aspergillus* and *Fusarium* species showed complete inhibition \approx 36 h. In the SNPs treated set of fungi, *Pythium* I and *Fusarium* were shown to be completely inhibited at \approx 42 h. The other fungal subjects, *Pythium* II and *Aspergillus* was fully inhibited by \approx 30 h (Fig. 9).

Statistical analysis of time kill assay predicted the *P*-value of 0.000495 and 0.000462 for ZnONPs and SNPs respectively (both are \leq 0.05). The change in variance for time kill assay was found to be a function of the time of contact as indicated by the increased value of variance as the time increases and downfall observed at the highest (\approx 100%) removal or killing of fungal spores in the suspension. The statistical analysis thus validates the results of experimental results.

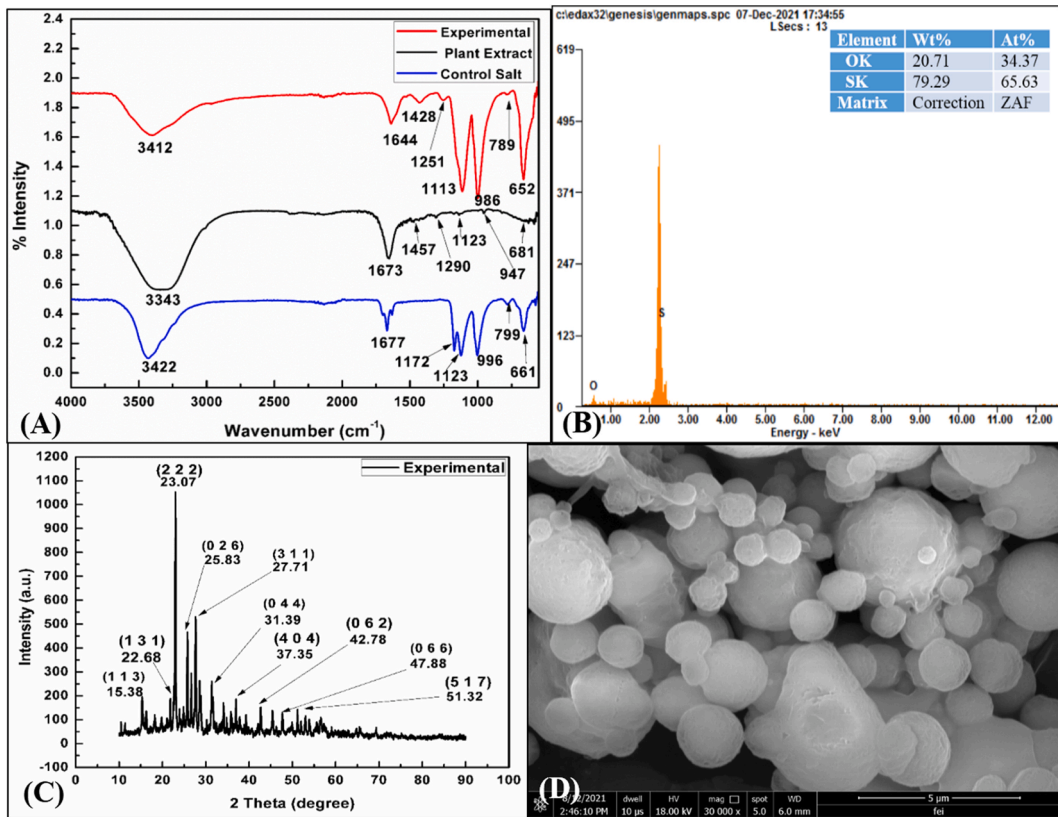


Fig. 6. Characterization of *M. oleifera* mediated SNPs, (A) Fourier Transform Infrared spectrum, (B) EDX pattern, (C) X-ray diffraction pattern, and (D) FESEM images.

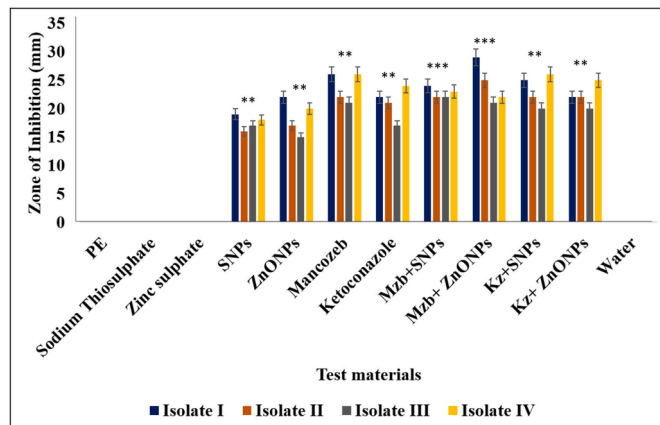


Fig. 7. Zones of inhibition against all the test fungi
Level of significance *** $P \leq 0.05$, NS = Non-significant.

4. Discussion

Ginger is globally consumed almost daily as a culinary spice as a fresh rhizome or in the form of a dried powder. It has medicinal properties as well as being an important spice cash crop its losses due to fungal infections need to be minimized. Authors chose to work under the growth inhibition of fungi that grow in ginger, because the fungi cause 60–90% losses in ginger post-harvest. The present study thus focused on developing a sustainable approach for management of deteriorating fungal pathogens in ginger and help farmers to enhance the crop conditions and crop yield in order to improve their economic status (Rai et al., 2018; Bazioli et al., 2019; Wang, 2020).

The phytopathogenic fungi isolated from soft-rot infected ginger were obtained in pure culture on PDA medium and were subjected to morphological microscopic examination. The morphological structures like the sizes, shapes, and locations of the sporangium on the mycelium, antheridium, oogonium and oospores were observed to identify the genus of given isolated fungi. The first

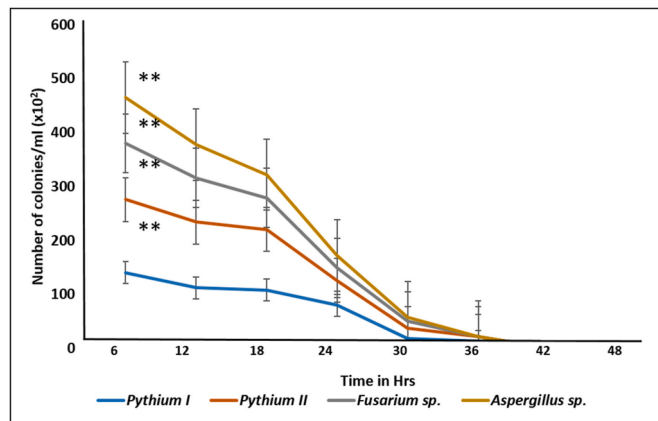


Fig. 8. Time kill assay of ZnONPs against all test isolates
Level of significance ** $P \leq 0.05$, NS = Non-significant.

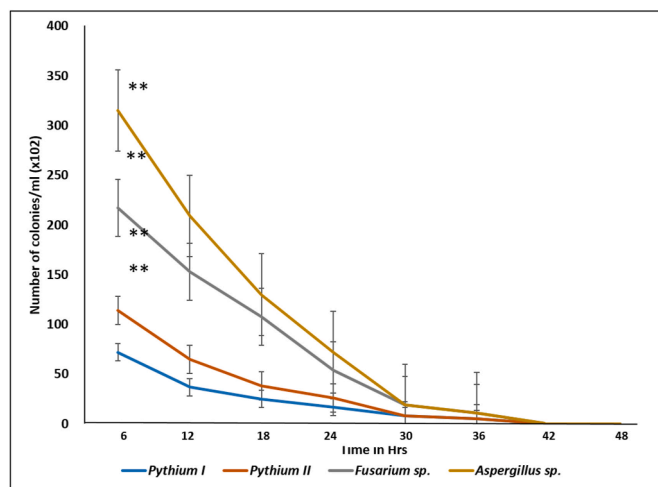


Fig. 9. Time kill assay of SNPs against all test isolates
Level of significance ** $P \leq 0.05$, NS = Non-significant.

two isolates were showing filamentous (thread-like), coenocytic (non-septate threads lacking cross walls) cell growth, which is a peculiar characteristic of *Pythium* spp. The asexual or vegetative stage of *Pythium* produces thick walled resting stage i.e. chlamydospores, as shown in Fig. 1 A. the standard key given by Dick (1990) was referred to identify the genus of the given isolates. On the basis of monograph (Van der Plaats-Niterink, 1981) of *Pythium* the isolate I and II (Fig. 1 A and B) were confirmed to belong to genus *Pythium*. The third isolate (III) was identified as a species of *Fusarium* genus (Fig. 1 C), an important phytopathogen associated with the soft-rot in ginger (Li et al., 2014; Rai et al., 2018). It was reported that the *Fusarium* can cause rhizome rot in ginger for the first time in China. Rhizome rot infected cultivar Laiwu Big Ginger, was reported in Anqiu, Shandong Province, with yield losses of up to 70% due to *Fusarium oxysporum* associated (Li et al., 2014; Prasath et al., 2023; Kaningini et al., 2023). Finally, the fourth isolate i.e. isolate IV, was found to belong to another major genus of phytopathogenic fungi i.e. *Aspergillus* (Fig. 1 D). The genus was determined based on *Aspergillus* manual by Thom and Raper (1945).

In the present study, *M. oleifera* aqueous extract was used for the synthesis of NPs because they are rich in various bioactive secondary metabolites, such as zeatin, caffeoylquinic acid, quercetin, kaempferol, and b-sitosterol, etc. Many of the reported metabolites are growth regulators, insecticides and are fungicidal in nature (Nizioł-Lukaszewska et al., 2020; Jenish et al., 2022). The huge array of compounds with *in vitro* antifungal, antiviral, antibacterial and antioxidant properties present in moringa extract, improves shelf life of crops and their high antioxidant concentration allows its preferential use over other plants. The ease of cultivation of moringa plants in temperate regions of Indian subcontinent is another advantage (Mncube et al., 2021; Oniha et al., 2021; Baldisserotto et al., 2023; Yadav et al., 2023b). It is observed that there is a significant decrease in the phytochemical constitution of moringa leaves during drying depending on the mode of drying i.e. freeze, air, sun or oven drying. On the contrary, fresh leaf extracts show higher contents of components like flavonoids, saponins, phenolics, vitamins, etc. That are most probably lost during drying. These phytochemicals play an important role during the synthesis and stabilization of nanoparticles. Hence, it is recommended to preferentially use the fresh leaf extract for nanoparticle synthesis due to its higher phytochemical composition. Moringa leaf extracts (fresh) was utilized in

the present study as it is rich in several antifungal compounds such as tannins and flavonoids that have already demonstrated inhibitory activity against fungi (Yadav et al., 2023b). This makes moringa as a suitable candidate to be used in the synthesis of antifungal nanoparticles (Ademiluyi et al., 2018; Rajput, 2017; Vergara-Jimenez et al., 2017). This suggests the use of moringa extract as a stabilizing agent and reducing material for the synthesis of antifungal nanoparticles. Various modes of antifungal materials are responsible for imparting fungicidal activity to the nanoparticles synthesized. Further, the zinc oxide nanoparticle synthesis by *M. oleifera* was confirmed with the formation of white colored colloid (Fig. 2 B) after addition of a few drops of alkali (0.1 N NaOH). The synthesis from aqueous extract of moringa leaves as a capping material stabilized the ZnONPs in the colloidal state. The spectrometric measurement showed absorption maxima at 356 nm (Fig. 3 A), which is an excellent match with the earlier report and within the range of typical Surface Plasmon Resonance Band for metal oxide NPs without any kind of aggregation (Venkatesham et al., 2012; Duque et al., 2019; Githala and Trivedi, 2023). The absorption maxima is an attribute of their huge excitation binding energy. The blue-shifted absorption spectrum and larger particle size is a function of quantum imprisonment effect exhibited by colloidal zinc nanomaterials (Abel et al., 2021; Degefa et al., 2021; Hazaa et al., 2021). The nanoparticle tracking analysis revealed the size and distribution of ZnONPs determined on the basis of their Brownian motion. Fig. 3 B and 3 D, revealed the average size of ZnONPs as 78 nm, with standard deviation of indicating polydispersed nanoparticle formation by moringa extract and distribution over a broad size range with very less amount of NPs with larger size (Jadhao et al., 2020; Irfan et al., 2021). The zeta potential of -14.1 mV and a single narrow peak revealed the stable nature of ZnONPs (Fig. 3 C), due to the stabilization of NPs by numerous metabolites present in the moringa extract. The high negative value indicated the stable ZnONPs which bypassed aggregation at room temperature in a colloidal state. The zeta potential values shown thus corroborated with the earlier studies based upon theories of stability of hydrophobic colloids (Derjaguin and Landau, 1941; Verwey and Overbeek, 1948). The stability of the synthesized NPs can be explained on the basis of presence of various biomolecules as predicted by Fourier Transform Infrared spectrometry (Fig. 4 A), in terms of percent transmittance and respective wavenumber (cm^{-1}) assigned to specific functional groups in the capping layer of NPs. The presence of transmittance bands assigned to $-\text{OH}$ group, aldehydic $\text{C}=\text{O}$ stretch, NO_2 group, and the $\text{C}-\text{Cl}$ stretch of chloro compounds probably contributed the negative value of zeta potential and the aliphatic $\text{C}-\text{H}$ stretch have formed the core of ZnONPs. The strong peaks between 400 and 600 cm^{-1} indicated the presence of metal oxides in the sample, confirming the presence of Zn-O stretching vibrations and formation of zinc oxide NPs (Matinise et al., 2017; Balan et al., 2019; Espenti et al., 2020; Mondal et al., 2024). In case of calcined ZnONPs the results are similar with the formation of prominent peaks in the range of 400–600 cm^{-1} (Adam et al., 2021). EDX analysis of ZnONPs (Fig. 4 B) represented the presence of major peaks for percent weight of Zn and oxygen, along with the smaller peaks belonging to the traces of impurities belonging to other elements. The lower atomic percent yield can be stipulated due to presence of Zn ions primarily in the core of NPs and outer surface is covered with the metabolites from the moringa extract. The results were in accordance with the previous reports by Ansari and colleagues (2020) and Espenti et al. (2020). The peculiar diffraction peaks in XRD spectrum (Fig. 4 C) of ZnONPs at Miller indices of 101, 102, 110, and 103 indicated the presence of face centered cubic crystal formation (JCPDS- File No. 89–0510). The sample showed the other minor peaks might be due to the formation of polymorphic ZnONPs crystals as represented in SEM images at 30000x resolution (Fig. 4 D). The SEM images signifies polymorphic nature of ZnONPs showing firstly the discoid crystals and secondly the multifaceted cuboidal diamond shaped crystals. This clarifies the variation in the size range of ZnONPs. Quartz like and disc shaped polymorphic crystals of ZnONPs were confirmed by FESEM images (Irfan et al., 2021). The disc like depositions of ZnONPs were reported previously which also showed the similar results as quoted in the present study (Abel et al., 2021). The size of ZnONPs was below 100 nm i.e. 78 nm (Iranbakhsh et al., 2021). As per the literature available, there are various modes of antifungal activity of nanoparticles has been reported. This includes the adsorption of NPs on the cell surface leading to membrane depolarization. Endocytosis of NPs ultimately results in cytosolic release of NMs and triggers the release of various reactive oxygen species (Lipovsky et al., 2011). On the other hand diffusion of NPs through the cell wall may also result in the intracellular damage including the damage to genetic material of the cell. This ultimately decides the fate of the cell to undergo the process of apoptosis, and death of the cell. Fig. 10 below represents the probable mechanism of antifungal activity of nanoparticles (Gurunathan et al., 2022).

Sulfur being an important element in soil is widely used in industry, pharmaceutical and agriculture as well. It is used as an active component of nitrogenous fertilizer. Sulfur is a key prosthetic group in many of the enzymes, co-enzymes and proteins. It also helps plants in mitigating biotic stress and disease resistance (Dubuis et al., 2005; Najafi et al., 2020; Kaur et al., 2023; Bhaskar et al., 2023). A green synthesis of Sulfur NPs had previously been reported by various methods using many kinds of plant extracts and without application of any hazardous additives (Banerjee and Rajeswari, 2024). In present study extract of fresh leaves of moringa plants were used to synthesize SNPs. Other researchers have confirmed the synthesis from various parts of plants like, fresh and dried leaves, fruits, bark and peels. Other plants explored for the biogenic synthesis of SNPs are *Alianthus altissima*, *Albizia julibrissin*, *Azadirachta indica*, *Cinnamomum zeylanicum*, *Punica granatum*, *Sophora japonica*, etc. (Ghotekar et al., 2020). Sodium thiosulphate is a common precursor material used for the plant mediated synthesis of SNPs. Synthesis of SNPs using sodium thiosulphate and bark extract of *Cinnamomum zeylanicum* resulted in formation of yellow colored precipitate (Najafi et al., 2020).

The absorption maxima of SNPs i.e. 295 nm (Fig. 5 A), was reported to be in the same range of wavelength as reported by Paralikar and Rai (2018). A study by Chaudhuri and Paria (2011), elaborated the growth kinetics in aqueous medium for SNPs that has similar absorption range. Further analysis of SNPs by NTA reported the size in the range below 100 nm. In NTA particles are sized one-by-one under laser light according to their Brownian motion in the area focused. The mean displacement is calculated for the particles moving in the same planes (Paralikar and Rai, 2018). NTA also predicted the crowding of SNPs more frequently in the range between 10 and 60 nm as per the 2D distribution graph (Fig. 5 D). Negative zeta potential values indicated null negative charge on the surface of the SNPs and the average zeta potential value away from zero viz. -21.2 mV (Fig. 5 C) indicated the stability of SNPs in colloidal systems. The FTIR spectrum of SNPs showed overlapping peaks in approximately the same wavenumber range as control i.e. *M. oleifera*

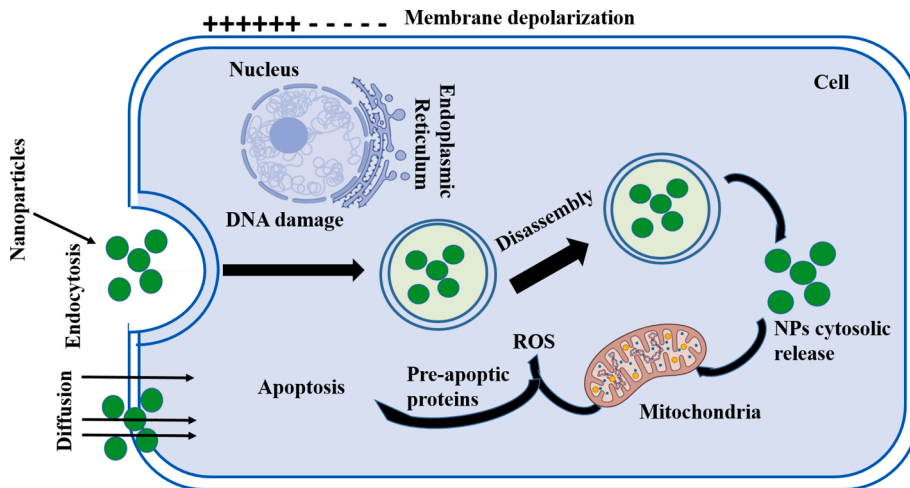


Fig. 10. Mechanism of antifungal activity of nanoparticles, Nanoparticles inhibit growth of fungal cell by entering into cell by endocytosis, release ROS and ultimately kills the cell by apoptosis.

extracts. Negative zeta potential supported the presence of negatively charged biomolecules from extract in the capping layer of SNPs (Coates, 2006; Choudhury et al., 2013). This confirms the presence of functional groups that are common to both, SNPs and control samples. The crystal lattice of SNPs was compared with the standard dataset. This indicated the SNPs with lattice corresponding to the JCPDS file No. 08247. The assigned peaks were presenting the structure of SNPs and the unassigned peaks in XRD were considered due to the impurities and amorphous matters in the test sample (Suleiman et al., 2013; Awwad et al., 2015; Suleiman et al., 2015). Majority of the SNPs reported are spherical, which supports the present findings. The results obtained from FESEM were analogous with the previous reported studies (Kouzegaran and Farhadi, 2017; Khairan et al., 2019; Ghotekar et al., 2020). The previous reports also supports the synthesis of spherical SNPs (Tripathi et al., 2018; Baloch et al., 2023). EDX analysis showed a higher percentage of sulfur in the matrix followed by oxygen (Ismalita et al., 2022).

The FESEM imaging as shown in Fig. 4 D and 6 D shows, that both the nanoparticles have distinct morphologies. The variation in the morphology of ZnONPs and SNPs is probably due to the difference in the reduction rate because of the presence of different biomolecules in moringa extract which are responsible for the different nucleation rates of the nanoparticle growth during the synthesis process. The reduction and stabilization of NPs by different biomolecules from moringa extract will decide the nanoparticle morphology and stability. Also, the nanoparticles' shape and size are defined by the surface energy required which is attended for electro- and thermodynamic stability during their stabilization (Pinchuk and Schatz, 2008; Yao et al., 2015; Vollath et al., 2018; Anand et al., 2020).

Several studies have shown the promising antifungal and antibacterial property of biogenic SNPs. For example, *Catharanthus roseus* extract mediated green synthesized SNPs were potential antifungal agents against *Microsporum canis* (Chantongsri et al., 2021). In the present study, the antifungal activity of SNPs was confirmed by visible inhibition of visible fungal growth on PDA plates. Larger zones of inhibition indicated the higher fungicidal potential of SNPs. MIC i.e. minimum inhibitory concentration was considered as the lowest concentration where visible fungal growth inhibition is observed on PDA plates with nitrocellulose plate loaded with the SNPs. In the present study both the nanoparticles i.e. ZnONPs and SNPs individually as well as synergistic activity in combination with fungicide mancozeb and antibiotic ketoconazole showed significant fungicidal activity against test fungi. This indicated the enhanced fungicidal effect of standard antifungal agents.

In time kill assay for ZnONPs and SNPs, time dependent antifungal activity was observed i.e. as the time of nanoparticle exposure to fungus increases the viable spore count as well as the colony count decreases. The earlier reports also suggests that enhancement of antifungal activity of SNPs was possibly due to the *C. roseus* extract which was used for their synthesis (Chantongsri et al., 2021; Abdel-Maksoud et al., 2023). Similarly, in the present study *M. oleifera* leaf extract was used which contains secondary metabolites which were the primary reason for stabilization of SNPs increasing surface to volume ratio. Here, both the nanoparticles ZnONPs and SNPs were thoroughly washed to remove any residual components from the moringa extract. This indicated the antifungal activity of the NPs was not the direct function of extract, instead the secondary metabolites involved in their stabilization. The fungal load decreased as the time of exposure with NPs increases. Thus, the fungal load was minimized at 42 and 36 h after exposure with ZnONPs and SNPs (Figs. 8 and 9). The results were in cohesion with the reports of Chantongsri et al. (2021) and Mohammed and Hawar (2022). The antifungal activity of NPs was an attribute of their small particle size, higher surface area to volume ratio which facilitates the adhesion as well as entry of NPs into the fungal mycelium. Thus rupturing the cell membrane and decreasing the integrity of the cell wall may be due to the decreased lipid content (Roy Chaudhary et al., 2013; Mohammed et al., 2022; Mahmud et al., 2023).

The synthesized ZnONPs and SNPs showed significant antifungal activity and will aid in formulation of nano-based fungicides. Various methods are available for the preparation of nanoformulations, and can be applied by various modes such as sprays, dusting, soil applicants, etc. Mode of application will differ based upon the desired activity of the nanoformulations. Nanoformulations developed by biological approach and a green methods will be more beneficial and economic with respect to their scaling up and public

use. But, before their agriculture application, there is a need for thorough field trials, and pilot scale studies followed by the large-scale field experimentation in natural environment (Krishnamoorthy and Mahalingam, 2015). The present study was aimed to evaluate *in vitro* antifungal potential of two nanoparticles ZnONPs and SNPs against fungal pathogens from ginger. This approach of applying two or more antifungal nanoparticles with variable biochemical composition (as elucidated by FTIR analysis) will minimize the risk of development of resistance and effective killing and management of fungal pathogens in the agricultural fields (Alghuthaymi et al., 2021).

In addition to the fungicidal potential of NPs, composition as well as chemical and biological properties of soil are greatly affected by the application and accumulation of the NPs. This may impact the microbial ecosystem of soil which plays an important role in the soil fertility maintenance. Uncontrolled dispersal and accumulation of various NPs will change the microbial and functional diversity of the soil. Thus controlled and more supervised application of NMs in agriculture is recommended (Ghidan and Al Antary, 2020; Chauhan, 2023). NMs can increase soil fertility significantly. But on the other hand, excess amounts can contaminate the soil, and finally migrate to ground waters. To prevent the damage to aquatic systems by rainwater runoff and soil erosion along with the transportation of the manufactured NMs from production sites is recommended (Ray et al., 2009). In order to prevent these complexities, it is advised to use NMs as per the recommendations of government agencies and in approved limits. Thorough field trials, *in vitro* and *in vivo* studies based upon the dose-dependent activities for their beneficial as well toxicity aspects will be required in the future to examine and anticipate the highest potential of NMs in agriculture (Tarafdar, 2015; DBT, 2020; Kalia et al., 2020; Cruz-Luna et al., 2021).

5. Conclusion

India being an agriculture-based country, it is important to fulfill the ever increasing requirements of food and feed. At the same time, it is required to follow safe practices for food production, storage and consumption. This can only be achieved through increased production and reduced pest infestation using a sustainable approach. Nanobiotechnology has proven its record as a new generation of a sustainable approach to mitigate problems in various fields including pharmaceutical, medicine, agricultural, etc. ZnONPs and SNPs reported in the present study were synthesized by a plant-based method. The phyto-stabilization of ZnONPs and SNPs was possible using *M. oleifera* crude leaf extract. The ZnONPs and SNPs were biologically synthesized, which makes them easily available for interaction with fungal counterparts and timely killing the target fungus. It can be concluded that the *in vitro* antifungal assessment of ZnONPs and SNPs against fatal phytopathogenic fungi of ginger such as, *Aspergillus*, *Fusarium* and *Pythium* signifies their application in development of alternative fungicidal materials for agricultural application can be produced and applied on a commercial scale for the pre-treatment of seed ginger before sowing. It can be concluded from the statistical analysis that, the significant inhibition of the fungal growth was observed with the increase in time of contact between fungal species with ZnNPs as well as SNPs. This will aid in the preparation of nanoformulation based upon these tested NPs against tested pathogenic fungal isolates from ginger, which can be publicly distributed after critical laboratory and field-based studies. The majority of the NPs are reported for their novel benefits in various fields like medicine and agriculture. However, their overuse may impose serious threats to the plants reducing the germination rate, bioaccumulation and environmental toxicity. It is thus necessary to evaluate their toxicity prior to public use based on the guidelines and standard application methods which will benefit farmers.

CRedit authorship contribution statement

Pramod U. Ingle: Writing – review & editing, Writing – original draft, Methodology, Investigation, Formal analysis, Data curation. **Mahendra Rai:** Visualization, Validation, Supervision, Project administration, Formal analysis, Data curation, Conceptualization. **Patrycja Golińska:** Writing – review & editing, Writing – original draft, Methodology, Investigation, Formal analysis. **Aniket K. Gade:** Visualization, Validation, Supervision, Project administration, Formal analysis, Data curation, Conceptualization.

Declaration of competing interest

Authors declare that they have no known competing financial interests or personal relationships that could have appeared to influence the work reported in this paper.

Data availability

Data will be made available on request.

Acknowledgement

PG and AKG would like to acknowledge this research as part of the project No. UMO-2022/45/P/NZ9/01571 co-funded by the National Science Centre and the European Union Framework Programme for Research and Innovation Horizon 2020 under the Marie Skłodowska-Curie grant agreement No. 945339. For the purpose of Open Access, the author has applied a CC-BY public copyright licence to any Author Accepted Manuscript (AAM) version arising from this submission.

Appendix A. Supplementary data

Supplementary data to this article can be found online at <https://doi.org/10.1016/j.bcab.2024.103229>.

References

- Abdel-Maksoud, G., Abdel-Nasser, M., Hassan, S.E.D., Eid, A.M., Abdel-Nasser, A., Fouda, A., 2023. Biosynthesis of titanium dioxide nanoparticles using probiotic bacterial strain, *Lactobacillus rhamnosus*, and evaluate of their biocompatibility and antifungal activity. *Biomass Conv. Bioref.* <https://doi.org/10.1007/s13399-023-04587-x>.
- Abel, S., Leta Tesfaye, J., Nagaprasad, N., Shanmugam, R., Priyanka Dwarampudi, L., Krishnaraj, R., 2021. Synthesis and characterization of zinc oxide nanoparticles using moringa leaf extract. *J. Nanomater.* <https://doi.org/10.1155/2021/4525770>. Article ID 4525770, 6.
- Adam, F., Himawan, A., Aswad, M., Ilyas, S., Heryanto, Anugrah, M.A., Tahir, D., 2021. Green synthesis of zinc oxide nanoparticles using *Moringa oleifera* water extract and its photocatalytic evaluation. *J. Phys. (Paris): Conference Series* 1763 (1), 012002. <https://doi.org/10.1088/1742-6596/1763/1/012002>.
- Adegboye, M., 2011. Evaluation of farmers' response to extension services on ginger production in Kagarko local government area of Kaduna State. *Sci. Res. Essays* 6 (6), 1166–1171. <https://doi.org/10.5897/SRE09.447>.
- Ademiluyi, A.O., Aladeselu, O.H., Oboh, G., Boligon, A.A., 2018. Drying alters the phenolic constituents, antioxidant properties, α -amylase, and α -glucosidase inhibitory properties of *Moringa (Moringa oleifera)* leaf. *Food Sci. Nutr.* 6, 2123–2133. [10.1002%2Ffn3.770](https://doi.org/10.1002%2Ffn3.770).
- Ahmadu, T., Ahmad, K., Ismail, S.I., Rashed, O., Asib, N., Omar, D., 2021. Antifungal efficacy of *Moringa oleifera* leaf and seed extracts against *Botrytis cinerea* causing gray mold disease of tomato (*Solanum lycopersicum* L.). *Braz. J. Biol.* 81(4), 1007–1022. <https://doi.org/10.1590/1519-6984.233173>. PMID: 33175006.
- Alghuthaymi, M.A., Rajkuberan, C., Rajiv, P., Kalia, A., Bhardwaj, K., Bhardwaj, P., Abd-Elsalam, K.A., Valis, M., Kuca, K., 2021. Nanohybrid antifungals for control of plant diseases: current status and future perspectives. *J. Fungi. (Basel)*. 7 (1), 48. <https://doi.org/10.3390/jof7010048>. PMID: 33450851; PMCID: PMC7828323.
- Anand, S., Pandiyan Kuppusamy, R.R., Padmanabhan, P., 2020. Insight into the kinetically and thermodynamically controlled biosynthesis of silver nanoparticles. *IET Nanobiotechnol.* 14 (9), 864–869. <https://doi.org/10.1049/iet-nbt.2019.0373>.
- Awad, M.F., Albogami, B., Mwabvu, T., Hassan, M.M., Baazeem, A., Hassan, M.M., Elsharkawy, M.M., 2023. Identification and biodiversity patterns of *Aspergillus* species isolated from some soil invertebrates at high altitude using morphological characteristics and phylogenetic analyses. *PeerJ* 11, e15035. <https://doi.org/10.7717/peerj.15035>.
- Awwad, A.M., Salem, N.M., Abdeen, A.O., 2015. Novel approach for synthesis sulfur (S-NPs) nanoparticles using *Albizia julibrissin* fruits extract. *Adv. Mater. Lett.* 6 (5), 432–435.
- Balan, V., Mihai, C.T., Cojocar, F.D., Uritu, C.M., Dodi, G., Botezat, D., Gardikiotis, I., 2019. Vibrational spectroscopy fingerprinting in medicine: from molecular to clinical practice. *Materials* 12, 2884. <https://doi.org/10.3390/ma12182884>.
- Baldissarotto, A., Barbari, R., Tupini, C., Buzzi, R., Durini, E., Lampronti, I., Manfredini, S., Baldini, E., Vertuani, S., 2023. Multifunctional profiling of *Moringa oleifera* leaf extracts for topical application: a comparative study of different collection time. *Antioxidants* 12, 411. <https://doi.org/10.3390/antiox12020411>.
- Baloch, H., Siddiqua, A., Nawaz, A., Latif, M.S., Zahra, S.Q., Alomar, S.Y., Ahmad, N., Elsayed, T.M., 2023. Synthesis and characterization of sulfur nanoparticles of *Citrus limon* extract embedded in nanohydrogel formulation: in vitro and in vivo studies. *Gels* 9, 284. <https://doi.org/10.3390/gels9040284>.
- Banerjee, M., Rajeswari, V.D., 2024. Green synthesis of selenium nanoparticles using leaf extract of *Moringa oleifera*, their biological applications, and effects on the growth of *Phaseolus vulgaris*: agricultural synthetic biotechnology for sustainable nutrition. *Biocatal. Agric. Biotechnol.* 55, 102978. <https://doi.org/10.1016/j.bcab.2023.102978>.
- Bauer, A.W., Kirby, W.M., Sherris, J.C., Turck, M., 1966. Antibiotic susceptibility testing by a standardized single disk method. *Am. J. Clin. Pathol.* 45 (4), 493–496. PMID: 5325707.
- Bazioli, J.M., Belinato, J.R., Costa, J.H., Akiyama, D.Y., Pontes, J.G.D.M., Kupper, K.C., Augusto, F., De Carvalho, J.E., Fill, T.P., 2019. Biological control of citrus postharvest phytopathogens. *Toxins* 11, 460.
- Bennett, M.A., Callan, N.W., Fritz, V.A., 1991. Seed treatments for disease control. *Horti. Tech.* 1, 84–87.
- Bereswill, R., Golla, B., Strelke, M., Schulz, R., 2012. Entry and toxicity of organic pesticides and copper in vineyard streams: erosion rills jeopardise the efficiency of riparian buffer strips. *Agric. Ecosyst. Environ.* 146 (1), 81–92. <https://doi.org/10.1016/j.agee.2011.10.010>.
- Bhaskar, M., Kumar, A., Rani, R., 2023. Application of nano formulations in agriculture. *Biocatal. Agric. Biotechnol.* 54, 102934. <https://doi.org/10.1016/j.bcab.2023.102934>.
- Chantongsri, A., Phuektes, P., Borlace, G.N., Aiemaasard, J., 2021. Antifungal activity of green sulfur nanoparticles synthesized using *Catharanthus roseus* extract against *Microrosporium canis*. *Thai J. Vet. Med.* 51 (4), 705–713. <https://doi.org/10.14456/tjvm.2021.85>.
- Chaudhuri, R.G., Paria, S., 2011. Growth kinetics of sulfur nanoparticles in aqueous surfactant solutions. *J. Colloid Interface Sci.* 354, 563–569.
- Chauhan, N.S., 2023. The impact of nanoparticles in agriculture and soil: conclusion and future recommendations. In: Chauhan, N.S., Gill, S.S. (Eds.), *The Impact of Nanoparticles in Agriculture and Soil: Nanomaterial-Plant Interactions*. Elsevier Publications, Amsterdam, The Netherlands, pp. 403–408.
- Chérif, M., Menzies, J.G., Ehret, D.L., Bogdanoff, C., 1994. Yield of cucumber infected with *Pythium aphanidermatum* when grown with soluble silicon. *Hortic. Sci. (Stuttg.)* 29 (8), 896–897.
- Choudhury, S.R., Mandal, A., Chakravorty, D., Gopal, M., Goswami, A., 2013. Evaluation of physicochemical properties, and antimicrobial efficacy of monoclinic sulfur-nanocolloid. *J. Nano Res.* 15 (1491), 1–11.
- CLSI, 2021. <https://www.treata.academy/wp-content/uploads/2021/03/CLSI-31-2021.pdf>.
- Coates, J., 2006. Interpretation of infrared spectra, a practical approach. In: Meyers, R.A. (Ed.), *Encyclopaedia of Analytical Chemistry*. John Wiley & Sons Ltd, Newtown, USA, pp. 10815–10837.
- Cruz-Luna, A.R., Cruz-Martínez, H., Vásquez-López, A., Medina, D.I., 2021. Metal nanoparticles as novel antifungal agents for sustainable agriculture: current advances and future directions. *J. Fungi* 7 (12), 1033. <https://doi.org/10.3390/jof7121033>.
- Dake, G.N., 1995. Diseases of ginger (*Zingiber officinale* rose) and their management. *J. Spices Arom. Crops* 4 (1), 40–48.
- DBT (Department of Biotechnology, India), 2020. Guidelines for Evaluation of Nano-Based Agri-Inputs and Food Products in India.
- Degefa, A., Bekele, B., Jule, L.T., Fikadu, B., Ramaswamy, S., Dwarampudi, L.P., Nagaprasad, N., Ramaswamy, K., 2021. Green synthesis, characterization of zinc oxide nanoparticles, and examination of properties for dye-sensitive solar cells using various vegetable extracts. *J. Nanomater.* <https://doi.org/10.1155/2021/3941923>. Article ID 3941923, 9.
- Derjaguin, B., Landau, L., 1941. Theory of the stability of strongly charged lyophobic sols and of the adhesion of strongly charged particles in solutions of electrolytes. *Acta Phys. Chim. Sin.* 14, 633–662.
- Dewanarayana, T.B., Wimalaratana, W., 2018. Challenges and prospects of ginger farming in Sri Lanka with special reference to plogahawela divisional secretariat division. *ISSN. Int. J. Business, Econ. Law* 17 (3), 2289. 1552.
- Dick, M.W., 1990. *Keys to Pythium*. University of Reading, Reading, U. K.
- Dick, M.W., 2001. *Straminopilous Fungi*. Kluwer Academic Press, Netherlands.
- Dugan, M.F., 2006. *The Identification of Fungi: an Illustrated Introduction with Keys, Glossary, and Guide to Literature*. APS Press, USA.
- Duque, J.S., Madrigal, B.M., Riascos, H., Avila, Y.P., 2019. Colloidal metal oxide nanoparticles prepared by laser ablation technique and their antibacterial test. *Colloids Interfaces* 3 (1), 25.
- El-Gebaly, A.S., Sofy, A.R., Hmed, A.A., Youssef, A.M., 2024. Green synthesis, characterization and medicinal uses of silver nanoparticles (Ag-NPs), copper nanoparticles (Cu-NPs) and zinc oxide nanoparticles (ZnO-NPs) and their mechanism of action: a review. *Biocatal. Agric. Biotechnol.* 55, 103006. <https://doi.org/10.1016/j.bcab.2023.103006>.
- Espenti, C.S., Rama Krishna, A.G., Rami Reddy, Y.V., 2020. Green biosynthesis of ZnO nanomaterials and their anti-bacterial activity by using *Moringa oleifera* root aqueous extract. *SN Appl. Sci.* 2, 1424. <https://doi.org/10.1007/s42452-020-2945-3>.
- Flood, J., 2010. The importance of plant health to food security. *Food Secur.* 2, 215–231.
- Gautam, J., Mainali, R.P., 2016. Management of ginger rhizome fly (*Calobata* sp.) and associated rhizome rot (*Pythium* sp.). *World J. Agri. Res.* 4 (4), 128–131.
- Ghazy, N.A., Abd El-Hafez, O.A., El-Bakery, A.M., El-Geddawy, D.L.H., 2021. Impact of silver nanoparticles and two biological treatments to control soft rot disease in sugar beet (*Beta vulgaris* L.). *Egy. J. Biol. Pest Cont.* 31 (1), <https://doi.org/10.1186/s41938-020-00347-5>.
- Ghidan, A.Y., Al Antary, T.M., 2020. Applications of Nanotechnology in Agriculture. *IntechOpen*. <https://doi.org/10.5772/intechopen.88390>.

- Ghotekar, S., Pagar, T., Pansambal, S., Oza, R., 2020. A review on green synthesis of sulfur nanoparticles via plant extract, characterization and its applications. *Adv. J. Chem.*, Sec. B. 2 (3), 128–143. <https://doi.org/10.33945/SAMI/AJCB.2020.3.5>.
- Gikas, G.D., Parlakidis, P., Mavropoulos, T., Vryzas, Z., 2022. Particularities of fungicides and factors affecting their fate and removal efficacy: a review. *Sustainability* 14, 4056. <https://doi.org/10.3390/su14074056>.
- Githala, C.K., Trivedi, R., 2023. Review on synthesis method, biomolecules involved, size affecting factors and potential applications of silver nanoparticles. *Biocatal. Agric. Biotechnol.* 54, 102912. <https://doi.org/10.1016/j.cbab.2023.102912>.
- Gurunathan, S., Lee, A.R., Kim, J.H., 2022. Antifungal effect of nanoparticles against COVID-19 linked black fungus: a perspective on biomedical applications. *Int. J. Mol. Sci.* 23, 12526. <https://doi.org/10.3390/ijms232012526>.
- Hayles, J., Johnson, L., Worthley, C., Losic, D., 2017. Nanopesticides: a review of current research and perspectives. *New Pesticides and Soil Sensors* 193–225.
- Hazaa, M., Alm-Eldin, M., Ibrahim, A.E., Elbarky, N., Salama, M., Sayed, R., Sayed, W., 2021. Biosynthesis of silver nanoparticles using *Borago officinalis* leaf extract, characterization and larvicidal activity against cotton leaf worm, *Spodoptera littoralis* (Bosid). *Int. J. Trop. Insect Sci.* 41 (1), 145–156.
- He, L., Liu, Y., Mustapha, A., Lin, M., 2011. Antifungal activity of zinc oxide nanoparticles against *Botrytis cinerea* and *Penicillium expansum*. *Microsc. Res.* 166 (3), 207–215. <https://doi.org/10.1016/j.mires.2010.03.003>.
- Ho, H.H., 2018. The taxonomy and biology of *Phytophthora* and *Pythium*. *J. Bacteriol. Mycol.* 6 (1), 40–45.
- ICAR-IISR, 2013. VISION-2050, ICAR- IISR, Kozhikode. 673012. Kerala.
- ICAR-IISR-Annual Report, 2022.
- Iranbaksh, A., Ardebili, Z.O., Ardebili, N.O., 2021. Synthesis and characterization of zinc oxide nanoparticles and their impact on plants. In: Singh, V.P., Singh, S., Tripathi, D.K., Prasad, S.M., Chauhan, D.K. (Eds.), *Plant Responses to Nanomaterials: Recent Interventions, and Physiological and Biochemical Responses, Nanotechnology in Life Science*. Springer, Germany, pp. 33–93.
- Ismalita, K., Rahmi, R., Syaifulhalla, M., Indra, I., 2022. Green synthesis of sulfur nanoparticles using *Allium sativum*: its effects on the growth of *Pogostemon cablin* Benth. and the chemical characterization of the patchouli oil after being harvested. *Nanotech. Env. Engg.* 7. <https://doi.org/10.1007/s41204-022-00217-5>.
- Jadhao, A.D., Shende, S., Ingle, P., Gade, A., Hajare, S.W., Ingole, R.S., 2020. Biogenic synthesis of zinc oxide nanoparticles by *Bryophyllum pinnatum* and its acute oral toxicity evaluation in wistar rats. *IEEE Trans. NanoBioscience* 1. <https://doi.org/10.1109/tmb.2020.3014023>. 1.
- Jayashree, E., Kandianan, K., Prasath, D., Rashid, P., Sasikumar, B., Senthil Kumar, C.M., Srinivasan, V., Suseela Bhai, R., Thankamani, C.K., 2016. *Ginger-extension pamphlet*. Indian council of Agricultural Research 682, 1–12.
- Jenish, A., Ranjani, S., Hemalatha, S., 2022. *Moringa oleifera* nanoparticles demonstrate antifungal activity against plant pathogenic fungi. *Appl. Biochem. Biotechnol.* 194 (10), 4959–4970. <https://doi.org/10.1007/s12010-022-04007-2>. Epub 2022 Jun 8. PMID: 35674924.
- Kalia, A., Abd-Elsalam, K.A., Kuca, K., 2020. Zinc-based nanomaterials for diagnosis and management of plant diseases: ecological safety and future prospects. *J. Fungi* (Basel). 6 (4), 222. <https://doi.org/10.3390/jof6040222>. PMID: 33066193; PMCID: PMC7711620.
- Kaningingi, A.G., Motlhalamme, T., Cloete, K.J., More, G.K., Mohale, K.C., Maaza, M., 2023. Fe₂O₃ nanoparticles from *Athrixia phyllicoides* DC and their effect on *Cicer arietinum* L. growth performance. *Biocatal. Agric. Biotechnol.* 54, 102948. <https://doi.org/10.1016/j.cbab.2023.102948>.
- Kaur, H., Hussain, S.J., Mir, R.A., Verma, V.C., Naik, B., Kumar, P., Dubey, R.C., 2023. Nanofertilizers – emerging smart fertilizers for modern and sustainable agriculture. *Biocatal. Agric. Biotechnol.* 54, 102921. <https://doi.org/10.1016/j.cbab.2023.102921>.
- Khairan, K., Zahratruriaz, Jalil, Z., 2019. Green synthesis of sulphur nanoparticles using aqueous garlic extract (*Allium sativum*). *Rasayan J. Chem.* 12, 50–57.
- Khandelwal, N., Barbole, R.S., Banerjee, S.S., Chate, G.P., Biradar, A.V., Khandare, J.J., Giri, A.P., 2016. Budding trends in integrated pest management using advanced micro-and nano-materials: challenges and perspectives. *J. Environ. Manag.* 184, 157–169.
- Kifile, A., Bekele, A., Tefera, T., Alemu, D., Koomen, I., Diro, M., Nigusie, D., 2023. Importance of ginger in Ethiopia: recent trends and challenges. *Stichting wageningen research Ethiopia*. Addis Ababa 2023, 32. SWRE-RAISE-FS-23-009. <https://doi.org/10.18174/635326>.
- Kouzegaran, V.J., Farhadi, K., 2017. Green synthesis of Sulphur Nanoparticles assisted by a herbal surfactant in aqueous solutions. *Micro & Nano Lett.* 12, 329–334.
- Krishnamoorthy, K., Mahalingam, M., 2015. Selection of a suitable method for the preparation of polymeric nanoparticles: multi-criteria decision making approach. *Adv. Pharmaceut. Bull.* 5 (1), 57–67. <https://doi.org/10.5681/apb.2015.008>. Epub 2015 Mar 5. PMID: 25789220; PMCID: PMC4352224.
- Leslie, J.F., Summerell, B.A., 2006. *The Fusarium Laboratory Manual*, third ed. Blackwell publishing, Ames, IA, USA.
- Li, Y., Chi, L.D., Mao, L.G., Yan, D.D., Wu, Z.F., Ma, T.T., Guo, M.X., Wang, Q.X., Quyang, C.B., Cao, A.C., 2014. First report of ginger rhizome rot caused by *Fusarium oxysporum* in China. *Plant Dis.* 98 (2), 282. <https://doi.org/10.1094/pdis-07-13-0729-pdn>. 282.
- Lipovsky, A., Nitzan, Y., Gedanken, A., Lubart, R., 2011. Antifungal activity of ZnO nanoparticles—the role of ROS mediated cell injury. *Nanotechnology* 22 (10), 105101. <https://doi.org/10.1088/0957-4484/22/10/105101>.
- Luong, T.M., Huynh, L.M.T., Hoang, H.M.T., Tesoriero, L.A., Burgess, L.W., Phan, G.H.T., Davies, P., 2010. First report of *Pythium* root rot of chrysanthemum in Vietnam and control with metalaxyl drench. *Austins Plant Disease Notes* 5 (1), 51–54.
- Mahmad, A., Chua, L.S., Noh, T.U., Siew, C.K., Seow, L.J., 2023. Harnessing the potential of *Heterotrigma itama* propolis: an overview of antimicrobial and antioxidant properties for nanotechnology-Based delivery systems. *Biocatal. Agric. Biotechnol.* 54, 102946. <https://doi.org/10.1016/j.cbab.2023.102946>.
- Matinise, N., Fuku, X.G., Kaviyarasu, K., Mayedwa, N., Maaza, M., 2017. ZnO nanoparticles via *Moringa oleifera* green synthesis: physical properties & mechanism of formation. *Appl. Surf. Sci.* 406, 339–347. <https://doi.org/10.1016/j.apsusc.2017.01.219>.
- Mncube, C.N., Bertling, I., Yobo, K.S., 2021. Investigating the antifungal activity of moringa leaf extract against *Fusarium* dry rot *in vitro*. *Acta Hort.* 1306, 233–240. <https://doi.org/10.17660/ActaHortic.2021.1306.29>.
- Mohammed, A.B.A., Mohamed, A., Al-Naggar, N.E., Mehrous, H., Nasr, G.M., Abdella, A., Ahmed, R.H., Irmak, S., Elsayed, M.S.A., Selim, S., Elkesh, A., Alkhalifah, D.H.M., Hozzein, W.M., Ali, A.S., 2022. Antioxidant and antibacterial activities of silver nanoparticles biosynthesized by *Moringa oleifera* through response surface methodology. *J. Nanomater.* 15. <https://doi.org/10.1155/2022/9984308>. 9984308.
- Mohammed, G.M., Hawar, S.N., 2022. Green biosynthesis of silver nanoparticles from *Moringa oleifera* leaves and its antimicrobial and cytotoxicity activities. *Int. J. Biomat.* (IJB) 4136641. <https://doi.org/10.1155/2022/4136641>. PMID: 36193175; PMCID: PMC9526645.
- Mondal, A., Mukherjee, A., Pal, R., 2024. Phycosynthesis of nanoiron particles and their applications- a review. *Biocatal. Agric. Biotechnol.* 55, 102986. <https://doi.org/10.1016/j.cbab.2023.102986>.
- Moslem, M.A., Mashraqi, A., Abd-Elsalam, K.A., Bahkali, A.H., Elnagaer, M.A., 2010. Molecular detection of ochratoxigenic *Aspergillus* species isolated from coffee beans in Saudi Arabia. *Genet. Mol. Res.* 9 (4), 2292–2299. <https://doi.org/10.4238/vol9-4gmr943>.
- Mustafa, M., Azam, M., Bhatti, H.N., Khan, A., Zafar, L., Abbasi, A.M.R., 2023. Green fabrication of copper nano-fertilizer for enhanced crop yield in cowpea cultivar: A sustainable approach. *Biocatal. Agric. Biotechnol.* 56, 102994. <https://doi.org/10.1016/j.cbab.2023.102994>.
- NAIP, 2014. National Agricultural Innovation Project, ICAR, A Value Chain on Ginger & Ginger Products. Orissa University of Agriculture & Technology, Odisha.
- Najafi, S., Razavi, S.M., Khoshkam, M., Asadi, A., 2020. Effects of green synthesis of sulfur nanoparticles from *Cinnamomum zeylanicum* barks on physiological and biochemical factors of Lettuce (*Lactuca sativa*). *Physiol. Mol. Biol. Plants* 26 (5), 1055–1066. <https://doi.org/10.1007/s12298-020-00793-3>. Epub 2020 Apr 18. PMID: 32377053; PMCID: PMC7196604.
- Navi, S.S., Huynh, T., Mayers, C.G., Yang, X.B., 2019. Diversity of *Pythium* spp. associated with soybean damping-off, and management implications by using foliar fungicides as seed treatments. *Phytopath. Res.* 1 (1). <https://doi.org/10.1186/s42483-019-0015-9>.
- Nejad, S.M., Najafabadi, N.S., Aghighi, S., Zargar, M., 2023. Phytosynthesis of silver nanoparticles by *Paulownia fortunei* fruit exudates and its application against *Fusarium* sp. causing dry rot postharvest diseases of banana. *Biocatal. Agric. Biotechnol.* 54, 102949. <https://doi.org/10.1016/j.cbab.2023.102949>.
- Nevedo-Velasquez, P.A., Ramirez - Gil, J.G., Garcia, G., Castellanos, D.A., Lopera, A.A., Bezvon, V.D.N., Paucar, C., 2023. Synthesis and application of Ag-doped TiO₂ nanoparticles with antifungal activity and ethylene inhibition in postharvest of avocado cv. Hass. *Biocat. Agri. Biot.* 54, 102901. <https://doi.org/10.1016/j.cbab.2023.102901>.
- Nizioł-Lukaszewska, Z., Furman-Toczek, D., Bujak, T., Wasilewski, T., Hordyjewicz-Baran, Z., 2020. *Moringa oleifera* L. extracts as bioactive ingredients that increase safety of body wash cosmetics. *Dermatol. Res. Practice* 8197902. <https://doi.org/10.1155/2020/8197902>.
- Oniha, M., Eni, A., Akinola, O., Omonigbehin, E.A., Ahuekwe, E.F., Olorunshola, J.F., 2021. *In vitro* Antifungal Activity of Extracts of *Moringa oleifera* on Phytopathogenic Fungi Affecting Carica papaya. *Macedonian J. Med. Sci.* 9 (A), 1081–1085. [Internet]. <https://oamjms.eu/index.php/mjms/article/view/6794>.

- Paralikar, P., Rai, M., 2018. Bio-inspired synthesis of sulphur nanoparticles using leaf extract of four medicinal plants with special reference to their antibacterial activity. *IET Nanobiotechnol.* 12 (1), 25–31. <https://doi.org/10.1049/iet-nbt.2017.0079>.
- Parveen, T., Sharma, K., 2014. Management of “soft rot” of ginger by botanicals. *Int. J. Pharm. Life Sci.* 5 (4), 3478–3484.
- Prasath, D., Matthews, A., O'Neill, W.T., Aitken, E.A.B., Chen, A., 2023. Fusarium yellows of ginger (*Zingiber officinale* roscoe) caused by *Fusarium oxysporum* f. sp. *zingiberi* is associated with cultivar-specific expression of defense-responsive genes. *Pathogens* 12 (1), 141. <https://doi.org/10.3390/pathogens12010141>. PMID: 36678490; PMCID: PMC9863783.
- Pinchuk, A.O., Schatz, G.C., 2008. Nanoparticle optical properties: far- and near-field electrodynamic coupling in a chain of silver spherical nanoparticles. *Mater. Sci. Eng. B* 149 (3), 251–258. <https://doi.org/10.1016/j.mseb.2007.09.078>.
- Rafique, K., Rauf, C.A., Naz, F., Shabbir, G., 2015. DNA sequence analysis, morphology and pathogenicity of *Fusarium oxysporum* f. sp. *lentis* isolates inciting lentil wilt in Pakistan. *Int. J. Biosci.* 7 (6), 74–91. <https://doi.org/10.12692/ijb/7.6.74-91>.
- Rajput, H., 2017. Chemical and phytochemical properties of fresh and dried *Moringa olifera* (PKM-1) leaf powder. *Chem. Sci. Rev. Lett.* 6 (22), 1004–1009. . Article CS132048042.
- Rai, M., Ingle, A.P., Paralikar, P., Anasane, N., Gade, R., Ingle, P., 2018. Effective management of soft rot of ginger caused by *Pythium* spp. and *Fusarium* spp.: emerging role of nanotechnology. *Appl. Microbiol. Biotechnol.* 102 (16), 6827–6839. <https://doi.org/10.1007/s00253-018-9145-8>.
- Raper, K.B., Fennell, D.I., 1965. *The Genus Aspergillus*. Williams & Wilkins, Baltimore.
- Ray, P.C., Yu, H., Fu, P.P., 2009. Toxicity and environmental risks of nanomaterials: challenges and future needs. *J. Environ. Sci. Health C Environ. Carcinog. Ecotoxicol. Rev.* 27 (1), 1–35. <https://doi.org/10.1080/10590500802708267>. PMID: 19204862; PMCID: PMC2844666.
- Sales, M.D.C., Costa, H.B., Fernandes, P.M.B., Ventura, J.A., Meira, D.D., 2016. Antifungal activity of plant extracts with potential to control plant pathogens in pineapple. *Asian Pac. J. Trop. Biomed.* 6, 26–31.
- Samson, A.R., Houbraken, J., Thrane, U., Frisvad, C.J., Andersen, B., 2009. In: Knaw, C.B.S. (Ed.), *Food and Indoor Fungi*. Fungal Biodiversity centre, Utrecht, The Netherlands.
- Sharma, S., Kumari, P., Thakur, P., Brar, G.S., Bouqellah, N.A., Hesham, A.E., 2022. Synthesis and characterization of Ni_{0.5}Al_{0.5}Fe₂O₄ nanoparticles for potent antifungal activity against dry rot of ginger (*Fusarium oxysporum*). *Sci. Rep.* 12, 20092. <https://doi.org/10.1038/s41598-022-22620-3>.
- Sivakumar, S., Sadaiyandi, V., Swaminathan, S., Ramalingam, R., 2024. Biocompatibility, anti-hemolytic, and antibacterial assessments of electrospun PCL/collagen composite nanofibers loaded with *Acanthophora spicifera* extracts mediated copper oxide nanoparticles. *Biocatal. Agric. Biotechnol.* 55, 102983. <https://doi.org/10.1016/j.bcab.2023.102983>.
- Suleiman, M., Al Ali, A., Hussein, A., Hammouti, B., Hadda, T.B., Warad, I., 2013. Sulfur nanoparticles: synthesis, characterizations and their applications. *J. Mater. Environ. Sci.* 4 (6), 1029–1033.
- Suleiman, M., Masri, M.A., Ali, A.A., Aref, D., Hussein, A., Sadeddin, I., Warad, I., 2015. Synthesis of nano-sized sulfur nanoparticles and their antibacterial activities. *J. Mater. Environ. Sci.* 6 (2), 513–518.
- Thom, C., Raper, K.B., 1945. *A Manual of the Aspergilli*. The Williams and Wilkins company, Baltimore.
- Tandon, A., Singh, A., Thakur, A., Sharma, V., 2023. Nanomaterial mediated genome engineering for sustainable food production: current status and future prospects. *Biocatal. Agric. Biotechnol.* 54, 102891. <https://doi.org/10.1016/j.bcab.2023.102891>. 2023.
- Tarafdar, J.C., 2015. Nanoparticle production, characterization and its application to horticultural crops. Winter School on “Utilization of Degraded Land and Soil through Horticultural Crops for Agricultural Productivity and Environmental Quality. December 3-23, 2015 at ICAR-National Research Centre on Seed Spices, Tabiji-305206, Ajmer, Rajasthan.
- Tilahun, S., Alemu, M., Tsegaw, M., Berhane, N., 2022. Morphological and molecular diversity of ginger (*Zingiber officinale* roscoe) pathogenic fungi in chilga district, north gondar, Ethiopia. *Front. Fungal Biol* 2, 765737. <https://doi.org/10.3389/ffunb.2021.765737>.
- Tripathi, R., Rao, R., Tsuzuki, T., 2018. Green synthesis of sulfur nanoparticles and evaluation of their catalytic detoxification of hexavalent chromium in water. *RSC Adv.* 8 (63), 36345–36352. . 10.1039%2Fc8ra07845a.
- Van der Plaats-Niterink, A.J., 1981. Monograph of the genus *Pythium*. Studies in Mycology. Baarn, Central bureau voor Schimmel cultures. Monograph No. 21, 242.
- Vergara-Jimenez, M., Almatrafi, M.M., Fernandez, M.L., 2017. Bioactive components in *Moringa oleifera* leaves protect against chronic disease. *Antioxidants* 6, 91. <https://doi.org/10.3390/antiox6040091>.
- Venkatesham, M., Ayodhya, D., Madhusudhan, A., Veerabhadram, G., 2012. Synthesis of stable silver nanoparticles using gum acacia as reducing and stabilizing agent and study of its microbial properties: a novel green approach. *Int. J. Green Nanotechnol.* 4 (3), 199–206.
- Verwey, E.J.W., Overbeek, J.T.G., 1948. *Theory of the Stability of Lyophobic Colloids*. Elsevier Publications, Amsterdam, The Netherlands.
- Vollath, D., Fischer, F.D., Holec, D., 2018. Surface energy of nanoparticles – influence of particle size and structure. *Beilstein J. Nanotechnol.* 9, 2265–2276. <https://doi.org/10.3762/bjnano.9.211>.
- Wang, H., 2020. Introductory Chapter: Studies on Ginger. *IntechOpen*. <https://doi.org/10.5772/intechopen.89796>.
- Yadav, D., Gaurav, H., Yadav, R., Waris, R., Afzal, K., Chandra Shukla, A., 2023a. A comprehensive review on soft rot disease management in ginger (*Zingiber officinale*) for enhancing its pharmaceutical and industrial values. *Heliyon* 9 (7), e18337. <https://doi.org/10.1016/j.heliyon.2023.e18337>. PMID: 37539157; PMCID: PMC10395546.
- Yadav, S., Goswami, P., Mathur, J., 2023b. Evaluation of fungicidal efficacy of *Moringa oleifera* Lam. leaf extract against *Fusarium* wilt in wheat 4, 100034. <https://doi.org/10.1016/j.napere.2023.100034>.
- Yao, Y., Wei, Y., Chen, S., 2015. Size effect of the surface energy density of nanoparticles. *Surf. Sci.* 636, 19–24. <https://doi.org/10.1016/j.susc.2015.01.016>.
- Ying, S., Guan, Z., Ofoegbu, P.C., Clubb, P., Rico, C., He, F., Hong, J., 2022. Green synthesis of nanoparticles: current developments and limitations. *Environ. Technol. Innov.* 26, 102336. <https://doi.org/10.1016/j.eti.2022.102336>.
- Zakir, M., Hailemichael, G., Seyoum, M., Addisu, M., 2018. Status of ginger (*Zingiber officinale*) research and production challenges and future prospects in Ethiopia; a review. *Acad. Res. J. Agri. Sci. Res.* 6 (5), 276–290. <https://doi.org/10.14662/ARJASR2018.027>.
- Zubrod, J.P., Bundschuh, M., Arts, G., Brühl, C.A., Imfeld, G., Knäbel, A., Payraudeau, S., Rasmussen, J.J., Rohr, J., Scharfmüller, A., Smalling, K., Stehle, S., Schulz, R., Schäfer, R.B., 2019. Fungicides: an overlooked pesticide class? *Environ. Sci. Technol.* 53 (7), 3347–3365. <https://doi.org/10.1021/acs.est.8b04392>.